The power of shallow-depth Toffoli and qudit quantum circuits

Alex B. Grilo[1], Elham Kashefi[1,2], Damian Markham[1], Michael de Oliveira[1,3,*]

[1]*Sorbonne Université, CNRS, LIP6, France*
[2]*School of Informatics, University of Edinburgh, Scotland*
[3] *International Iberian Nanotechnology Laboratory, Portugal*

Abstract

The relevance of shallow-depth quantum circuits has recently increased, mainly due to their applicability to near-term devices. In this context, one of the main goals of quantum circuit complexity is to find problems that can be solved by quantum shallow circuits but require more computational resources classically.

Our first contribution in this work is to prove new separations between classical and quantum constant-depth circuits. Firstly, we show a separation between constant-depth quantum circuits with quantum advice $\mathsf{QNC}^0/\mathsf{qpoly}$, and $\mathsf{AC}^0[p]$, which is the class of classical constant-depth circuits with unbounded-fan in and $\pmod{p}$ gates. In addition, we show a separation between QAC^0, which additionally has Toffoli gates with unbounded control, and $\mathsf{AC}^0[p]$. This establishes the first such separation for a shallow-depth quantum class that does not involve quantum fan-out gates.

Secondly, we consider QNC^0 circuits with infinite-size gate sets. We show that these circuits, along with (classical or quantum) prime modular gates, can implement threshold gates, showing that $\mathsf{QNC}^0[p] = \mathsf{QTC}^0$. Finally, we also show that in the infinite-size gateset case, these quantum circuit classes for higher-dimensional Hilbert spaces do not offer any advantage to standard qubit implementations.

---

[*]✉ michael.oliveira@inl.int

1 Introduction

In the current landscape dominated by NISQ (Noisy Intermediate-Scale Quantum) devices [34], understanding the computational power of shallow-depth quantum circuits has both practical and theoretical relevance. From a practical perspective, given the noisy aspect of near-term devices, focusing on tasks that achieve quantum advantage in low depth is fundamental. From a theoretical perspective, (classical) constant-depth circuits have been crucial in the development of lower bound techniques, e.g. [39]. Thus, the combination of these techniques, along with the computational capabilities of constant-depth quantum circuits, enables the discovery of new quantum-classical separations and, furthermore, allow a more comprehensive understanding of quantum computational complexity classes [40, 24, 19].

The holy-grail in quantum circuit complexity is to find problems that can be solved by shallow-depth quantum circuits and that cannot be solved by polynomial-time classical computation. Unfortunately, there are several caveats in the current approaches. Firstly, the current super-polynomial quantum advantage proposals rely on computational assumptions, offering no unconditional proof of quantum superiority. Secondly, some of these results even require quantum gates with arbitrary accuracy, which cannot be implemented in practice in real-world devices. This problem is amplified when infinite gate sets are assumed [9, 3], since it has been shown that even if precise quantum operations were feasible, the computational overhead for classical control could destroy any quantum advantage [23].

More recently, there is a new line of research that has addressed some of these issues, at the cost of achieving weaker statements. More concretely, the seminal work of [6] has shown a problem that can be solved by constant-depth quantum circuits (QNC^0), and which cannot be solved by constant-depth classical circuits with bounded fan-in (NC^0). We would like to highlight that while this separation is weaker (since the lower bound is only against constant depth circuits), it is *unconditional*, which is rather rare in complexity theory. Moreover, these proposals also have practical interest with their extension to include fault-tolerance [7].

The result of [6] has also been extended to achieve better quantum/classical separations: We currently have separations between quantum constant-depth circuits and constant-depth classical circuits with *unbounded fan-in* (AC^0), even if the classical circuit has access to (mod 2) gates ($\mathsf{AC}^0[2]$) [44].[1] In these results, showing the quantum upper bound is fairly easy and the main difficulty is in the classical lower bound. The main challenge lies in finding new classical lower bounds techniques that allow us answer the question:

What is the largest class of classical circuits that we can separate from constant-depth quantum circuits?

The main contribution of this work is to prove new separations between constant-depth quantum circuits and constant-depth classical circuits. Additionally, we revisit quantum circuits with infinite gateset and prove new collapses of different quantum circuit classes.

1.1 Our contributions

Our first contribution is showing that a set of relation problems for which we have constant-depth quantum circuits on qudits with quantum advice and is not contained in $\mathsf{AC}^0[p]$.

Result 1. *(Informal; see Theorem 17) For all primes p, there exists a finite gate set on qudits of dimension p such that constant-depth quantum circuits with quantum advice can solve relation problems that are intractable for any polynomial-size $\mathsf{AC}^0[p]$ circuit, i.e., $\mathsf{QNC}^0_p/\mathsf{qpoly} \nsubseteq \mathsf{AC}^0[p]$.*

---

[1]We notice that in order to prove the separation against classical circuits with parity gates, the quantum circuit has access to quantum advice.

This result extends the $\mathsf{AC}^0[2]$ separation from [44] to general primes. To prove it, we generalize the relation problems on modular operations that have been used in [6, 44]. Roughly, our modular relation problems with parameters $p, q \in \mathbb{N}$ consist of a pair of bit strings (x, y) such that $|x|$ (mod p) = 0 iff $|y|$ (mod q) = 0. Here, $|x|$ and $|y|$ represent the Hamming weights of the respective bit strings. We show that by exploiting higher-dimensional gate sets, we can solve these problems in constant-depth quantum circuits with a copy of a high-dimensional GHZ state. At the same time, we expand the classical lower bound to $\mathsf{AC}^0[p]$. However, this separation achieves only a quantum/classical distinction regarding error probabilities, which differ by a constant value. In order to improve these separations, we then consider the parallel repetition of these modular problems as proposed in [44, 13]. In our results, we simplify the proof of [44] by considering the one-sided error of the quantum circuits and using "seminal results" in circuit complexity such as the Vazirani XOR lemma [16] and Razborov-Smolensky separations [41].

We follow by showing that QAC^0 circuits, without quantum fanout gates but permitting the fanout of classical information, can generate high-dimensional GHZ states. For this, we employ optimal depth and size methods for GHZ state creation, which is based on poor-man's cat states and balanced binary trees as the resource state entanglement structure. This gadget, along with Result 1, allows us to show that for every prime p, there exists a constant-depth quantum circuit employing Toffoli gates of dimension p that computes a relation unattainable by any polynomial-size $\mathsf{AC}^0[p]$ circuit. Moreover, when Toffoli gates of arbitrary arity can implement any qubit operation, we attain an unconditional separation between this complexity class and all $\mathsf{AC}^0[p]$ classes simultaneously. It is worth noting that this aligns with the standard definition of QAC^0 as outlined in existing literature [32, 38, 14, 4] while including classical and excluding quantum fanout, and that recent research and practical demonstrations have suggested that some platforms quantum devices inherently support multi-qubit operations which would enable the construction of multi-qubit Toffoli gates [28, 20, 21, 8].

Result 2. *(Informal; see Theorem 18) For every prime p, there is a relation problem that can be solved by QAC^0 circuits without quantum fanout, whereas any $\mathsf{AC}^0[p]$ circuit of polynomial size solves it with a negligible probability. Therefore, $\mathsf{QAC}^0 \nsubseteq \mathsf{AC}^0[p]$ holds for all prime p.*

This establishes the first separation between QAC^0 and $\mathsf{AC}^0[p]$ for any prime p, which was recently asked in [38]. We notice that in order to achieve such a result with our techniques, it is crucial to consider qudits of higher dimensions. Additionally, we remark that QAC^0 can generate a GHZ state without the need for unbounded parity gates, as proposed in [38]. Our QAC^0 circuits use quantum measurements and adaptive operations to generate the quantum states. Surprisingly, the capability to produce this state does not imply the capability to compute the parity function. We conjecture that generating the GHZ state through a unitary procedure (i.e. without measurements) would require quantum fanout or parity gates. Thus, the question of whether the parity function can be computed in QAC^0 without fanout gates remains open for further investigation [30].

Next, we provide some limitations on our techniques by showing a classical upper bound on the modular relation problems that we consider.

Result 3. *(Informal; see Lemma 19) For every primes p, q, the modular relation problem on strings (x, y) such that $|x|$ (mod p) = 0 iff $|y|$ (mod q) = 0 can be solved by $\mathsf{NC}^0[q]$ circuits.* [2]

We notice that this result was unknown even for $p = 2$ and it characterizes $\mathsf{AC}^0[p]$ as the largest constant-depth classical circuit class for which a quantum-classical separation can be identified using our proposed relation problems. To achieve separations against classes like TC^0 (or larger classes), one needs to consider a different class of problems such as [19]. However, it is conjectured that this particular set of modular relation problems is sufficient to achieve unconditional separations

---

[2]These circuits are composed of bounded fan-in gates, as in NC^0, but additionally contain a single unbounded fan-in MOD_p gate.

between the aforementioned $\mathsf{AC}^0[p]$ classical circuit classes and less powerful quantum circuit classes, such as QNC^0.

We then switch gears and consider the class of constant-depth quantum circuits with an infinite gateset and multi-qudit fanout.[3] In this setting, we show that for any prime p, we have the collapse of the constant-depth quantum hierarchy for quantum circuits with p-dimensional qudits, extending the qubit case [42].

Result 4. *(Informal; see Theorem 27) For all prime p, there exists an infinite gate set on qudits of dimension p such that constant depth quantum circuits built with this gate set and unbounded fan-in* MOD_p *gates implement quantum threshold gates in constant depth, i.e.,* $\mathsf{i\text{-}QNC}^0_p[p] = \mathsf{i\text{-}QTC}^0_p.$[4]

This result establishes computational equivalence across shallow-depth quantum circuits when implemented on systems over prime-dimensional Hilbert spaces. Specifically, our quantum circuits are constructed using Fourier transforms over Abelian groups and this approach allows the creation of circuits for functions over finite fields of the form $\mathbb{F}_p^n \to \mathbb{F}_p$. These circuits allow the execution of multi-qubit controlled logical operations.

Subsequently, we show that constant-depth quantum circuits implemented in higher prime dimensions can be implemented with qubits with a multiplicative overhead. This highlights that for any algorithm falling within these classes, employing qudits instead of qubits offers no substantial computational benefits—except perhaps for more straightforward hardware implementations and better error-correcting schemes in Hilbert spaces of varying dimensions.

Result 5. *(Informal; see Theorem 30). For all primes p and q, any constant depth quantum circuit with gates on qudits of dimension p and quantum threshold gates can be replicated by a constant-depth quantum circuit over qubits, with access to classical* MOD_q *gates,* $\mathsf{i\text{-}QTC}^0_p \subseteq \mathsf{i\text{-}QNC}^0_2[q]_\mathsf{c}.$

This result is achieved by mapping qudit operations onto tensor products of qubits. The qudit operations are produced using exact unitary decomposition methods, as previously demonstrated for qubits [37, 2]. Specifically, this theorem implies that the qubit-specific hierarchy can be collapsed using any arbitrary classical modular prime gate — a capability previously believed to require either quantum fanout or multi-qubit parity gates. Consequently, we have that $\mathsf{QNC}^0[p]_\mathsf{c} = \mathsf{QACC}^0$ holds for all primes p. This significantly contrasts with classical analog circuit classes, where adding different modular gates results in different complexity classes.

From a practical standpoint, it also demonstrates that quantum circuits with fixed-depth qubits, when augmented with unbounded fan-in classical prime modular operations MOD_p, can implement the quantum subroutines of algorithms like factoring, which have been conjectured to convey exponential quantum advantage [22, 10].

Finally, we leave as future work to extend Result 5 and show that any $\mathsf{i\text{-}QTC}^0_p$ circuit can be simulated by $\mathsf{i\text{-}QNC}^0_q$ circuits with additional classical modular gates, for arbitrary primes p and q. This would establish the equivalence between all constant-depth quantum circuits over qudits of different prime dimensions.

1.2 Organization

Section 2 delves into the study of shallow-depth quantum circuits with finite-size gate sets. In this section, we introduce the concept of modular relation problems and elucidate how quantum circuits can solve these problems. Additionally, we establish the $\mathsf{AC}^0[p]$ lower bounds for the circuit classes addressing these problems and conclude the section by defining the $\mathsf{NC}^0[p]$ classical upper

---

[3]For any prime p, multi-qudit fanout for p-dimensional qudits is equivalent to MOD_p gates.

[4]As we describe later, in our notation, the prefix $i-$ denotes that the gate set is infinite, and the subscript p denotes that the qudits have dimension p. Additionally, $[p]$ means access to a quantum and $[p]_c$ to a classical unbounded fan-in modular p gate.

bounds for the relation problems under consideration. In Section 3, we shift our focus to constant-depth quantum circuits over qudits. This section explores the implications of employing infinite-size gate sets and unbounded fan-in modular gates, demonstrating both hierarchical collapses and computational equivalences between qubit and qudit formulations.

We assume readers have a basic understanding of qudit quantum computation, types of computational problems (such as decision, search, and sampling), and classical constant-depth circuits. For additional information, refer to Appendix A for an overview.

Acknowledgments

2 Shallow depth quantum circuits with finite-size gate sets

In this section, we show new separations between quantum shallow circuits and classical ones. More precisely in Section 2.1, we introduce the classes of quantum circuits considered in our work. Then, in Section 2.2, we prove the quantum upper bounds, and in Section 2.3, we prove the classical lower bounds. We combine these results in Section 2.4 in order to achieve our new separations. Finally, in Section 2.5, we discuss the limitations of our techniques.

2.1 Definitions

The initial circuit class under examination comprises a gate set defined by a finite collection of gates and is restricted to single qudit control gates, encompassing standard universal gate sets like the Clifford+T gate set.

Definition 1 (QNC_d^0). *For $d \in \mathbb{N}$, let $\mathcal{H}^d$ denote a d-dimensional Hilbert space. $\mathcal{G}_d$ being a finite set of quantum gates that operate on $\mathcal{H}^d$, while $\mathcal{C}_d$ represents a fixed number of gates that act on one qudit, controlled by another qudit. We define QNC_d^0 as the class of quantum circuits with constant depth and polynomial size, employing a gate set compiled from the combination of $\mathcal{G}_d$ and $\mathcal{C}_d$.*

The subsequent class to be analyzed will supplement the finite number of qudit gates with their multi-qudit controlled variants. This introduces an alternative characterization for the quantum counterpart of AC^0 that has not been addressed in prior literature and guarantees a fairer comparison between the quantum and classical constant-depth circuit classes.

Definition 2 (QAC_d^0). *For $d \in \mathbb{N}$, let $\mathcal{H}^d$ denote a d-dimensional Hilbert space. Let $\mathcal{G}_d$ represent a finite set of gates acting on $\mathcal{H}^d$, which are permitted unbounded classical fanout—defined as the ability to replicate a gate's output indefinitely, allowing its use as input for numerous other gates—when these gates are characterized as maps from basis states to basis states with classical inputs. Let $\mathcal{T}_d$ denote a fixed number of multi-qudit controlled gates acting on a single qudit. We define QAC_d^0 as the class of quantum circuits with a constant depth and polynomial size, using a gate set drawn from the combination of $\mathcal{G}_d$ and $\mathcal{T}_d$.*

In this work, we also consider the complexity classes $\mathsf{i\text{-}QNC}_d^0$ and $\mathsf{i\text{-}QAC}_d^0$. These variants of QNC_d^0 and QAC_d^0 incorporate the full set of one-qudit unitaries. We will provide a formal definition of these classes in Section A.3.

Additionally, we consider access to quantum advice, which is a quantum state that depends on the input size but not on the input. In particular, we consider $\mathsf{QNC}_d^0/\mathsf{qpoly}$, which consists of QNC_d^0 with a polynomial-size quantum advice.

We also examine extensions of certain constant-depth circuit classes, including unbounded fan-in modular operations. For example, the class $\mathsf{i\text{-}QNC}_d^0[p]$ integrates $\mathsf{i\text{-}QNC}_d^0$ circuits with an additional quantum modular gate defined as follows,

$$\mathsf{qMOD}_p \, |x_0, x_1, \ldots, x_n\rangle := |x_0 + (x_1 + \ldots + x_n) \mod p, x_1, \ldots, x_n \mod p\rangle. \tag{1}$$

Finally, we use the suffix $[p]_c$ to denote the inclusion of a classical unbounded fan-in modular gate MOD_p in these circuit classes.

We now define the notion of modular relation problems.

Definition 3 (Modular relation problem)**.** *The modular relations problem $\mathcal{R}_{q,p}^m : \{0,1\}^n \to \{0,1\}^m$ is defined as*

$$\mathcal{R}_{q,p}^m(x) = \left\{ y \mid y \in \mathbb{F}_2^m, \ |y| \pmod{q} = 0 \text{ iff } |x| \pmod{p} = 0 \right\}. \tag{2}$$

This class of problems subsumes the relation problem used in [6, 44], which uses $\mathcal{R}_{2,4}^{o(n^2)}$ for the NC^0 and the AC^0 separations, and [44], that uses $\mathcal{R}_{2,3}^{o(n^2)}$ for their $\mathsf{AC}^0[2]$ separation.

In this work, we also consider the parallel repetitions of these relation problems.

Definition 4 (Parallel-k modular relation problem)**.** *A modular relation problems $k\text{-}\mathcal{R}_{q,p}^m : \{0,1\}^{n \cdot k} \to \{0,1\}^{m \cdot k}$ are defined as,*

$$k\text{-}\mathcal{R}_{q,p}^m(x_1, ..., x_k) = \left\{ (y_1, ..., y_k) \mid \forall x_i \in \mathbb{F}_2^n, \ y_i \in \mathbb{F}_2^m, \ |y_i| \pmod{q} = 0 \text{ iff } |x_i| \pmod{p} = 0 \right\}.$$

Finally, we also define two key orthogonal bases for qudit states that will be used in our works. The first one is an extension of the qubit X-basis for qudits.

Definition 5 (Qudit orthogonal X-basis)**.** *The qudit orthogonal X-basis can be described by the set of states,*

$$|X_d^m\rangle = \frac{1}{\sqrt{d}} \sum_{j=0}^{d-1} \omega^{j \cdot m} |j\rangle \tag{3}$$

with $\omega = e^{\frac{i 2\pi}{d}}$ and $m \in \{0, 1, ..., d-1\}$.

The second orthogonal basis is tailored specifically for qudit GHZ states and will be necessary for the analysis of the quantum circuits we will present.

Definition 6 (Qudit-GHZ orthogonal X-basis)**.** *The qudit-GHZ orthogonal X-basis can be defined by the set of states,*

$$|\mathsf{GHZ}_{d,n}^m\rangle = \frac{1}{\sqrt{d}} \sum_{j=0}^{d-1} \omega^{j \cdot m} |j\rangle^{\otimes n} \tag{4}$$

with $\omega = e^{\frac{i 2\pi}{d}}$ and $m \in \{0, 1, ..., d-1\}$.

Finally, we state two technical lemmas regarding these bases that are needed in our results.

Lemma 7. $\langle X_d^m | X_d^n \rangle = \langle \mathsf{GHZ}_d^m | \mathsf{GHZ}_d^n \rangle = \delta_{m,n}$.

Proof. All the elements of the qudit orthogonal X-basis can be represented as,

$$|X_d^m\rangle = \frac{1}{\sqrt{d}} \sum_{i=0}^{d-1} \omega^{i \cdot m} |i\rangle = \mathsf{F}_d |m\rangle . \tag{5}$$

This yields that,

$$\langle X_d^m | X_d^n \rangle = \langle m | \mathsf{F}_d \mathsf{F}_d^\dagger | n \rangle . \tag{6}$$

Combining this with the fact that the $\mathsf{F}_d^\dagger \mathsf{F}_d |m\rangle = |m\rangle$, we obtain that $\langle X_d^m | X_d^n \rangle = \delta_{m,n}$. The same result holds for the qudit-GHZ orthogonal X-basis, given that the bases are simply a tensor product over n elements of the same bases as in the qudit X-basis. $\qquad \square$

Lemma 8. $\mathsf{F}_d^{\otimes n} |\mathsf{GHZ}_{d,n}^m\rangle = \frac{1}{\sqrt{d^{n-1}}} \sum_{\substack{x \in \mathbb{F}_d^n \\ |x| \mod d = -m}} |x\rangle.$

Proof. By considering the effect of the operator on the basis states we determine that,

$$\mathsf{F}_d^{\otimes n} |\mathsf{GHZ}_d^m\rangle = \frac{1}{\sqrt{d}} \sum_{i=0}^{d-1} \left(\omega^{i \cdot m} \mathsf{F}_d^{\otimes n} |i\rangle^{\otimes n} \right) \tag{7}$$

$$= \frac{1}{\sqrt{d}} \sum_{i=0}^{d-1} \omega^{i \cdot m} \left(\frac{1}{\sqrt{d^n}} \sum_{x \in \{0,1,\dots,d-1\}^n} \omega^{i \cdot |x|} |x\rangle \right) \tag{8}$$

$$= \frac{1}{\sqrt{d^{n+1}}} \sum_{x \in \{0,1,\dots,d-1\}^n} \sum_{i=0}^{d-1} \omega^{i \cdot (m+|x|)} |x\rangle \tag{9}$$

with $|x| = \sum_{i=0}^{n-1} x_i \mod d$. This implies that for all the inputs x for which $m + |x| \mod d = 0$ the value of $\omega^{i \cdot (m+|x|)} = 1$. In contrast, for inputs x for which $m + |x| \mod d \neq 0$ we will use the geometric progression to demonstrate first that the sum of all roots of unity is equal to zero,

$$\sum_{i=0}^{d-1} \omega^i = \frac{1 - \omega^d}{1 - \omega} = 0 . \tag{10}$$

Then, with one more step, we can show that the same is true for the amplitudes of the inputs considered,

$$\sum_{i=0}^{d-1} \omega^{i \cdot (m+|x|)} = \frac{1 - \omega^{d \cdot (m+|x|)}}{1 - \omega^{m+|x|}} = 0 . \tag{11}$$

Finally, this implies that only for values that $m + |x| \mod d = 0$ the amplitude of the respective basis states $|x\rangle$ are non-zero. This produces exactly the states,

$$\frac{1}{\sqrt{d^{n-1}}} \sum_{x \in X} |x\rangle, \ \textit{with } X = \left\{ y \mid y \in \{0, 1, \dots, d-1\}^n, |y| \mod d = -m \right\} . \tag{12}$$

$\qquad \square$

2.2 Quantum upper bounds

In this subsection, we introduce lower bounds for the probability that QNC^0 circuits with quantum advice and QAC^0 circuits can solve the modular relation problems.

2.2.1 Shallow depth quantum circuits with advice

In this subsection, we will introduce quantum circuits with a quantum advice that compute $\mathcal{R}_{q,p}^{q \cdot n}$ with a one-sided error.

Theorem 9. *For all fixed and distinct primes p and q, $\mathcal{R}_{q,p}^{q \cdot n}$ can be solved in $\mathsf{QNC}_q^0/\mathsf{qpoly}$ with one-sided error at most $\frac{1-\cos(\frac{2\pi}{p})}{q}$.*

Proof. The circuit for $\mathcal{R}_{q,p}^{q \cdot n}$ problem is described in Figure 1.

The initial state is $|x\rangle\,|\mathsf{GHZ}_{q,n}^0\rangle$, where the GHZ state is the quantum advice of the circuit. Then, we apply a layer of n control-Z rotations on the n qubits with a phase equal to $\frac{2\pi}{p}$. The i-th bit of the input x acts as the control qubit to the control-Z with the target being the i-th qubit of the GHZ state.

The first register is then

$$|\psi^{(1)}\rangle = \frac{1}{\sqrt{q}}\Big(\sum_{i=0}^{q-2}|i\rangle^{\otimes n} + e^{i\frac{2\pi|x|}{p}}|q-1\rangle^{\otimes n}\Big) = \sum_{i=0}^{q-1} c_i\,|\mathsf{GHZ}_{q,n}^i\rangle, \tag{13}$$

with the second equality being the decomposition of $|\psi^{(1)}\rangle$ in the qudit-GHZ orthogonal X-basis.

If we apply $F_q^{\otimes n}$ to $|\psi^{(1)}\rangle$, we have

$$|\psi^{(2)}\rangle = \mathsf{F}_q^{\otimes n}|\psi^{(1)}\rangle = \sum_{i=0}^{q-1} c_i\,(\mathsf{F}_q^{\otimes n}|\mathsf{GHZ}_{q,n}^i\rangle) = \sum_{i=0}^{q-1} c_i \sum_{\substack{z\in[q]^n \\ |z| \mod q = -i}} |z\rangle,$$

where the last equality comes from Lemma 8.

Our goal is to compute the probability of measuring this state and get an output y such that $|y| \pmod p = 0$. For that, notice that c_0 is:

$$\langle\mathsf{GHZ}_{q,n}^0|\psi^{(1)}\rangle = \frac{1}{\sqrt{q}}\sum_{i=0}^{q-1}\langle i|^{\otimes n}\frac{1}{\sqrt{q}}\Big(\sum_{i=0}^{q-2}|i\rangle^{\otimes n} + e^{i\frac{2\pi|x|}{p}}|q-1\rangle^{\otimes n}\Big) = \frac{q-1+\cos(\frac{2\pi|x|}{p})}{q}. \tag{14}$$

We then divide that analysis into two cases:

1. If $|x| \mod p = 0$, $(c_0)^2$ equals 1. Consequently, measuring $|\psi_2\rangle$ leads to a string y such that $|y| \mod q = 0$.

2. If $|x| \mod p \neq 0$, we have $c_0^2 \leq \frac{q-1+\cos(\frac{2\pi|x|}{p})}{q}$. This implies that with a probability of least $\frac{1-\cos(\frac{2\pi}{p})}{q}$, it holds that $|y| \mod q \neq 0$.

The remaining step consists of mapping $y \in [q]^n$ to bit-strings $y' \in \{0,1\}^{q \cdot n}$ such that the Hamming weight is preserved. This can be done with extra ancilla qubits by mapping each $y_i \in [q]$ to the bit-string $1^{y_i}0^{q-y_i}$. We denote the circuit that performs such an operation as $C(q,2)$. $\qquad\square$

2.2.2 Shallow depth quantum circuits with Toffoli gates

We show now that quantum circuits of constant depth built with multi-qudit controlled operations along with intermediate measurements can generate qudit-GHZ states, demonstrating that QAC_q^0 (without advice) can solve $\mathcal{R}_{q,p}^{q \cdot n}$ with a one-sided error.

To achieve these qudit GHZ states, we use a specialized entanglement structure built upon "poor-man's cat states," as referenced in [44, 3, 25]. Specifically, poor-man's cat states are formulated using graphs where the number of vertices is equal to the state's qubit count, and the edge configuration guarantees a unique path between all vertices. In our work, we fix this graph to balanced binary trees $\mathcal{B}_n$ and extend these quantum states to higher dimensions.
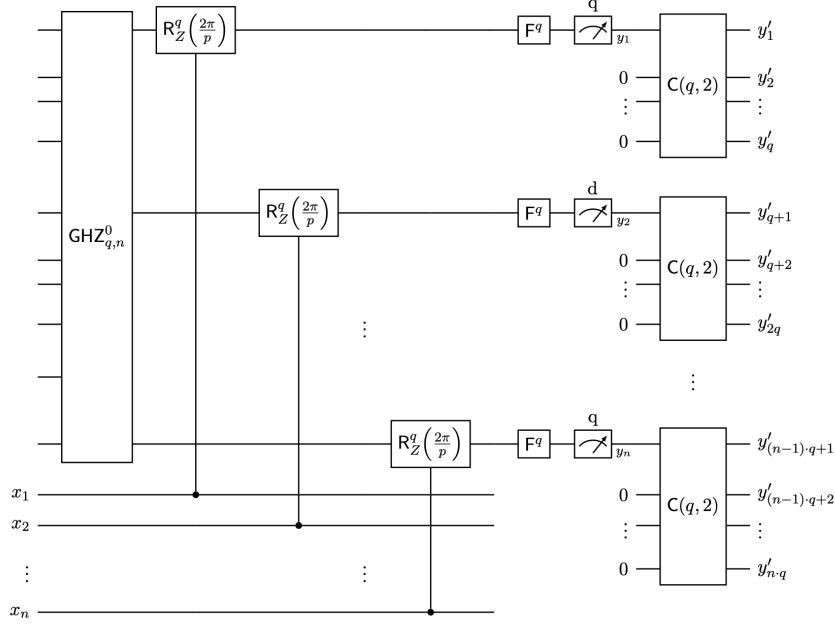
Figure 1: Parameterized quantum circuit class for values q, p, and n, incorporating the advice quantum state $|\mathsf{GHZ}_{q,n}^0\rangle$, which solves the $\mathcal{R}_{q,p}^{q \cdot n}$ with bounded one-sided error.

Definition 10 (Binary tree-structured poor-man's qudit state).)**.** *Let q be a prime. We consider the balanced binary tree $\mathcal{B}_n = (V, E)$, where $V = \{1, ..., n\}$ and $E = \{\{i, \lfloor \frac{i}{2} \rfloor\} : i \in \{2, ..., n\}\}$. As an example, we depict $\mathcal{B}_6$ in Figure 2.*

We define a binary tree-structured poor-mans qudit state $|\mathsf{BPM}_{q,n}\rangle$ as follows

$$|\mathsf{BPM}_{q,n}\rangle = \frac{1}{\sqrt{q^n}} \sum_{e_2, ..., e_n, v_1 \in \mathbb{F}_q} |e_2, ..., e_n\rangle |v_1, v_2, v_3, \ldots, v_n\rangle, \tag{15}$$

where each v_i, $i \in \{2, ..., n\}$ is recursively defined as

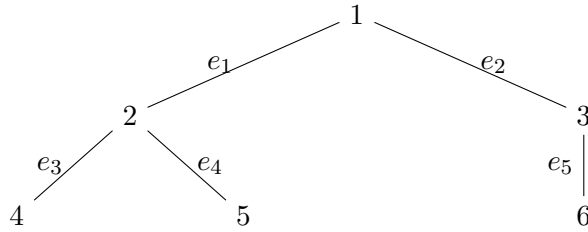$$v_i = e_i - v_{\lfloor \frac{i}{2} \rfloor}. \tag{16}$$

Figure 2: Representation of $\mathcal{B}_6$.

We now show that these states can be created using constant-depth quantum circuits.

Lemma 11. *For $n \in \mathbb{N}$, $|\mathsf{BPM}_{q,n}\rangle$ can be prepared in QNC_q^0.*

Proof. For creating this state, we start with a single qudit for each vertex and edge in $\mathcal{B}_n$, i.e., we have $|V| + |E|$ qudits, where the i-th qudit, for $1 \leq i \leq n-1$ corresponds to the edge $\{i+1, \lfloor \frac{i+1}{2} \rfloor\}$ and the i-th qudit, for $n \leq i \leq 2n-1$ corresponds to the vertex $i - n + 1$. We label qudits by their corresponding vertices/edges.

9

We start by applying the Fourier gate F_q to each of the vertex qudits and then, for edge $e = \{u, v\} \in E$ we apply a $\mathsf{SUM}_{u,e}$[5] and $\mathsf{SUM}_{v,e}$. The overall state after these operations is:

$$\sum_{v_1,\ldots,v_n\in\mathbb{F}_q} \frac{1}{\sqrt{q^n}} \left|(v_1+v_2),(v_1+v_3)...,(v_n+v_{\frac{n}{2}})\right\rangle \otimes |v_1,v_2,v_3,\ldots,v_n\rangle \tag{17}$$

$$= \sum_{e_1,v_1,v_3...,v_n\in\mathbb{F}_q} \frac{1}{\sqrt{q^n}} \left|e_1,(v_1+v_3)...,(v_n+v_{\frac{n}{2}})\right\rangle \otimes |v_1,e_1-v_1,v_3,\ldots,v_n\rangle \tag{18}$$

$$= \sum_{e_1,e_2,v_1,v_4...,v_n\in\mathbb{F}_q} \frac{1}{\sqrt{q^n}} \left|e_1,e_2...,(v_n+v_{\frac{n}{2}})\right\rangle \otimes |v_1,e_1-v_1,e_2-v_1,v_4,\ldots,v_n\rangle \tag{19}$$

$$... \tag{20}$$

$$\sum_{e_1,\ldots,e_{n-1},v_1\in\mathbb{F}_q} \frac{1}{\sqrt{q^n}} |e_1,...,e_{n-1}\rangle \otimes |v_1,e_1-v_1,e_2-v_1,\ldots,e_{n-1}-v_{\frac{n}{2}}\rangle \tag{21}$$

$$= |\mathsf{BPM}_{q,n}\rangle, \tag{22}$$

where all operations are (mod q) and all the equalities hold by rewriting the elements in $\mathbb{F}_q$.

Finally, given that the F_q gates are all applied in parallel to the vertex qudits, and the chromatic number of a balanced binary tree is equal to 3, all the $\mathsf{SUM}_{i,j}$ gates can be parallelized in order to be implemented in constant depth. $\qquad\square$

We now show that these states can be easily converted to GHZ states.

Lemma 12. *There is a QAC_q^0 circuit C_n that maps $|\mathsf{BPM}_{q,n}\rangle$ to the n-qudit state $|\mathsf{GHZ}_{q,n}^0\rangle$.*

Proof. In the circuit C_n, we first measure the edge qudits leading to the output string $e_1...e_{n-1} \in \mathbb{F}_q^{n-1}$. The collapsed quantum state is

$$|e_1,...,e_{n-1}\rangle \otimes \frac{1}{\sqrt{q}} \sum_{v_1\in\mathbb{F}_q} |v_1,v_2,...,v_n\rangle. \tag{23}$$

where $v_i = e_i - v_{\lfloor\frac{i}{2}\rfloor}$. Notice that by opening this recurrence relation, we have that

$$v_i = \sum_{j=0}^{depth(i)-1} (-1)^{depth(i)-depth(q^j(i))} e_{q^j(i)} + (-1)^{depth(i)+1} v_1, \tag{24}$$

where $depth(i)$ denotes the depth of node i in the tree and $q^j(i)$ denotes the j-th predecessor of i in the tree.

We notice that for each i, the value $c_i := \sum_{j=0}^{depth(i)-1} (-1)^{depth(i)-depth(q^j(i))} e_{q^j(i)}$ can be computed by $poly(n)$-size AC^0 circuits on input, since it depends on at most $\log(n)$ values e_j. In this case, a $poly(n)$-size AC^0 exists that computes $c_1...c_n$. Given these corrections, we can apply the gate X^{c_i} to the i-th vertex qubit (which is a classically-controlled X gate), and the resulting state is:

$$|e_1,...,e_{n-1}\rangle \otimes \frac{1}{\sqrt{q}} \sum_{v_1\in\mathbb{F}_q} \bigotimes_{i=1}^{n} |(-1)^{depth(i)}v_1\rangle. \tag{25}$$

Finally, we can apply the following operation to the qudits corresponding to the vertex of odd depth: $V|m\rangle = |p-m\rangle$ and the result state is

$$|e_1,...,e_{n-1}\rangle \otimes \frac{1}{\sqrt{q}} \sum_{v_1\in\mathbb{F}_q} |v_1\rangle^{\otimes n} \qquad\qquad\square.$$

---

[5]The $\mathsf{SUM}_{i,j}$ gate serves as the qudit equivalent of the CNOT gate and operates according to $\mathsf{SUM}_{i,j}|n\rangle_i|m\rangle_j = |n\rangle|n+m\rangle$.

The reduction we previously discussed cannot be achieved using QNC^0 or $\mathsf{i\text{-}QNC}^0$ circuits since they cannot implement the essential corrections needed to transition from the poor man's cat states to the GHZ states. In contrast, we explore the additional computational power of QAC^0 circuits and show that they can produce the qudit GHZ states through a process involving mid-circuit measurements. As a consequence, we can show the following.

Theorem 13. *For any distinct primes p and q, a QAC_q^0 circuit can solve $\mathcal{R}_{q,p}^{q \cdot n}$ with one-sided error at most $\frac{1 - \cos(\frac{2\pi}{p})}{q}$.*

Proof. Combining Lemma 11 and Lemma 12, we obtain that QAC_q^0 circuits can create qudit GHZ states of the type $|\mathsf{GHZ}_{q,n}^0\rangle$. In addition, all the QNC_q^0 circuits of Theorem 9 are contained in QAC_q^0. Therefore, all modular relation problems of the form $\mathcal{R}_{q,p}^{q \cdot n}$ fixed prime numbers p and q can be solved by QAC^0 circuits. □

2.3 Classical lower bounds

In this subsection, we prove the classical lower bounds for $\mathcal{R}_{p,q}^{q \cdot n}$. For that, we reduce it to computing MOD_p function and use the Razborov-Smolensky separations (Theorem 35) for $\mathsf{AC}^0[q]$. Then, we consider the $k\text{-}\mathcal{R}_{q,p}^{q \cdot n}$ problem, and we show that $\mathsf{AC}^0[q]$ circuits can solve them with only a negligible probability at best by using the Vazirani-XOR lemma.

Lemma 14. *Let p and q be two distinct primes. Any depth d circuit in $\mathsf{AC}^0[q]$ that solves the $\mathcal{R}_{q,p}^{q \cdot n}$ problem with one-sided error probability at most $1/n^{\Omega(1)}$ has size $\exp(n^{1/(2d - \Theta(1))})$.*

Proof. Let us suppose, for the purpose of a contradiction, that there exists a circuit C in $\mathsf{AC}^0[q]$ of depth $d - 3$ and size equal to $\exp(n^{1/(2d - \Theta(1))})$ that computes $\mathcal{R}_{q,p}^{q \cdot n}$, with one-sided error probability at most $\frac{1}{n^{o(1)}}$. We will assume here that C computes the yes-instance with probability 1, and the arguments follow analogously if C computed the no-instances with probability 1.

We will now prove that if such a C exists, then there exists a $\mathsf{AC}^0[q]$ circuit C' that computes the MOD_p function correctly with probability $1 - negl(n)$. C' consists of running $O(n^2)$ times the circuit C in parallel and then applying a MOD_q gate to each output string, and then applying a NOR gate to the output of this layer of MOD_q gates. Figure 3 provides a representation of C'.

If $|x| \mod p = 0$, after running C on x, the resulting strings y_i are such that $|y_i| \mod q = 0$. Thus, the MOD_q gates to each of these strings lead to output 0. Therefore, after the NOR gate, the result for this final bit will always be 1.

On the other hand, if $|x| \mod p \neq 0$, with probability $1/n^{o(1)}$, the strings y_i after running C have the desired property $|y_i| \mod q \neq 0$. Therefore, with the same probability, the MOD_q gate applied to this string will result in the Boolean value 1, and the probability of at least one of them being equal to 1 is at least $1 - negl(n)$. Therefore, the output of the NOR gate is 0 with probability $1 - negl(n)$.

This leads to a depth-d circuit and size $\exp(n^{1/(2d - \Theta(1))})$, that computes MOD_p in $\mathsf{AC}[q]$, contradicting Theorem 35. Thus, circuit C with such properties cannot exist. □

Subsequently, we show that polynomial-sized $\mathsf{AC}^0[q]$ circuits solve the parallel repetition of the modular relation problems with probability close to zero. To obtain this bound, we focus on the success of $\mathsf{AC}^0[q]$ circuits in computing the MOD_2 function with one-sided error.

Corollary 15. *The MOD_2 function can not be solved by any one-sided error $\mathsf{AC}^0[q]$ circuit with q prime $q \neq 2$ with a probability higher than $1/2 + 1/n^{\Omega(1)}$.*

Proof. Let's assume there exists an $\mathsf{AC}^0[p]$ circuit that can solve the Yes instances of the MOD_2 perfectly, then we know by Lemma 14 that the No instances can almost be solved correctly with probability $1/n^{o(1)}$. This implies any circuit of this type solves the MOD_2 function over a random input w.p. at most $1/2 + 1/n^{o(1)}$. □
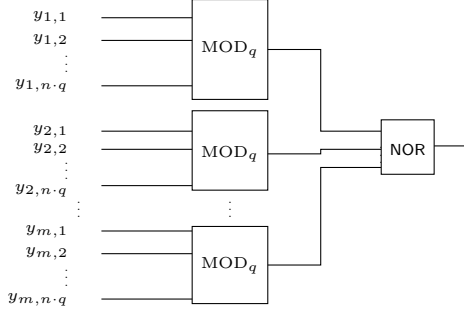
Figure 3: Representation of a classical $\mathsf{AC}^0[q]$ circuit, parameterized by q and n, that reduces a solution to the $\mathcal{R}^{q \cdot n}_{q,2}$ problem to a solution of $\mathrm{MOD}_2(x)$, where x is the initial input string of size n.

Using all these tools, we can show that the class of $\mathsf{AC}^0[q]$ fails to compute completely parallel modular relation problems with a one-sided error for some parameter regimes.

Lemma 16. *Let $q \neq 2$ be a prime and $k \in \Theta(\log(n))$. No $\mathsf{AC}^0[q]$ circuit can solve k-$\mathcal{R}^{q \cdot n}_{q,2}$ on at least $\frac{1}{2} + \frac{1 - \cos(\frac{2\pi}{p})}{2q}$ fraction of the parallel instances with one-sided errors and a probability higher then $n^{-\Omega(1)}$.*

Proof. Let us suppose that there exists a circuit $C \in \mathsf{AC}^0[q]$, where $q \neq 2$, can solve the k-$\mathcal{R}^{q \cdot n}_{q,2}$ with the properties of the statement. Then, we can construct a circuit C' that solves the following search problem

$$k\text{-}\mathcal{D}_{2,2}(x_1, ..., x_k) = \left\{ (y'_1, ..., y'_k) \; \middle| \; \forall x_i \in \mathbb{F}_2^n, \; y'_i \in \mathbb{F}_2, \; y'_i + |x_i| \pmod 2 = 0 \right\}, \tag{26}$$

with the same success, where C' is equal to C with an extra layer of MOD_q gates, thereby transforming the outcome strings from k-$\mathcal{R}^{q \cdot n}_{q,2}$ into bits using the mapping $\mathrm{MOD}_q(y_i) = y'_i$.

The circuit C' induces a probability distribution $\mathcal{X}$ on $\{0,1\}^k$, corresponding on picking random $x_1, ..., x_k \in \{0,1\}^n$ and outputting k output bits as follows,

$$(|x_1| + C'_1(x_1, \ldots, x_n) \pmod 2, ..., |x_k| + C'_k(x_1, \ldots, x_n) \pmod 2). \tag{27}$$

Our goal now is to prove that $\mathcal{X}$ is close to a uniform distribution $\{0,1\}^k$ on half of its bits, either for all x_i with even or odd Hamming weight, if we assume one-sided error. For that, we notice that we can describe for all $S \subseteq [k]$ the following expectation value as

$$\left| \mathbb{E}_{z \in \mathcal{X}}[(-1)^{\chi_S(z)}] \right| = \frac{1}{2^{|S| \cdot n}} \sum_{x_1, ..., x_k \in \mathbb{F}_2^n} (-1)^{\oplus_{i \in S}(|x_i| + C'_i(x_1, ..., x_n) \pmod 2)} \tag{28}$$

$$= \frac{1}{2^{|S| \cdot n}} \sum_{x_1, ..., x_k \in \mathbb{F}_2^n} (-1)^{\left(\sum_{i \in S} |x_i| + \sum_{i \in S} C'_i(x_1, ..., x_n) \right) \pmod 2}, \tag{29}$$

where $\chi_S(z) = \oplus_{i \in S} z_i$.

This allows us to bind the previous value for all the subsets S based on the number of times the following equation is fulfilled for uniformly selected strings x_i,

$$\sum_{i \in S} |x_i| \equiv \sum_{i \in S} C'_i(x_1, \ldots, x_n) \mod 2. \tag{30}$$

We observe that determining the values for the outcome bits $i \in S$ such that the condition of Equation (30) is satisfied by an $\mathsf{AC}^0[q]$ circuit C' is as hard as computing the parity function

across the concatenated input strings $||_{i \in S} x_i$. This assertion is supported by the fact that a circuit, which, if capable of determining valid outcome bits under the given condition, can be reduced to one that does compute the parity of the concatenated input strings $||_{i \in S} x_i$ with a polynomial-size $\mathsf{AC}^0[q]$ circuit. The latter follows from the fact that polynomial size $\mathsf{AC}^0[q]$ circuits can effectively compute the parity of a string of length $\log(n)$. Consequently, the probability that Equation (30) is satisfied is directly related to the probability that an $\mathsf{AC}^0[q]$ circuit computes the parity function across the concatenated input strings $||_{i \in S} x_i$, albeit with a one-sided error. This condition is met with a maximum probability of $1/2 + n^{-\Omega(1)}/2$, as inferred from Corollary 15. Therefore, we deduce that for any characteristic function χ_S, the value of $|\mathbb{E}_{x \in D}[(-1)^{\chi_S(x)}]|$ is limited by $\frac{1}{n^{\Omega(1)}}$, for all input strings of either even or odd Hamming weight.

Now, we can apply Vazirani's XOR Lemma (Lemma 38) to demonstrate that the distribution $\mathcal{X}$ is at most $1/n^{\Omega(1)} \cdot 2^{k/2}$ deviated in total variational distance from the uniform distribution, on those inputs. Then, we can show by using the Chernoff bound that the event X described as sampling a string with at least $1/2 + \frac{1 - \cos(\frac{2\pi}{p})}{2q}$ of 0's from this distribution, has a probability that decreases with,

$$\Pr\left(X\right) < e^{-2 \cdot (4 / \frac{1 - \cos(\frac{2\pi}{p})}{2q})^2 (1/2)^2 / (k^2)} < e^{-\Omega(k^2)} . \tag{31}$$

Thus, we obtain that the distribution $\mathcal{X}$ contains the same string with probability at most,

$$n^{-\Omega(1)} \cdot 2^{k/2} + e^{-\Omega(k^2)} = n^{-\Omega(1) + k/(2 \log(n))}. \tag{32}$$

Finally, we conclude that the previous value is bounded by $n^{\Omega(1)}$, given that $k = \log(n)$. $\qquad \square$

2.4 Separations

In this section, we combine the results from Section 2.2.1 and Section 2.3 to achieve unconditional separation between the classical and quantum circuit classes.

Theorem 17. *For each fixed prime q, there exists a relation problem that cannot be solved by polynomial-size circuits $\mathsf{AC}^0[q]$ with success probability at least $n^{-\Omega(1)}$, whereas there is a $\mathsf{QNC}^0_q/\mathsf{qpoly}$ circuit and a QAC^0_p circuit that can solve it with probability of least $1 - o(1)$.*

Proof. For the case where $q = 2$, the result is derived from Theorem 6 in [44]. For all $q \neq 2$, we apply the lower bounds and the respective instances of the parallel modular relation problems k-$\mathcal{R}^{q \cdot n}_{q,2}$ discussed in Lemma 16. These instances establish that $\mathsf{AC}^0[q]$ circuits solve this set of problems with a probability of at most $n^{-\Omega(1)}$.

In contrast, the $\mathsf{QNC}^0_q/\mathsf{qpoly}$ circuit, described in Theorem 9, can solve each instance of the parallel repetition game with a one-sided error of $\frac{1 - \cos(\frac{2\pi}{p})}{q}$. Similarly, QAC^0_p circuits achieve the same success probability, as detailed in Theorem 13. By combining these individual solutions, we deduce that the resulting global strategies effectively solve the k-$\mathcal{R}^{q \cdot n}_{q,2}$ problems, as outlined in Lemma 16, with a probability of at least $1 - o(1)$. This follows by considering their respective individual success probabilities and applying the Chernoff bounds. $\qquad \square$

Remark: We implicitly used the fact that the MOD_2 operation is not contained in any other $\mathsf{AC}^0[q]$ class with $q \neq 2$, which simplifies the proof since it allowed us to uniquely use Vazirani's XOR Lemma. However, we notice that the proof could follow with any other prime values and modular functions.

One drawback of the previous results is that we need to pick a different qudit dimension for each modular relation problem. However, if we consider infinite-size gatesets, we can show that all the previous quantum circuits can be implemented with qubits and prove the separation for $\mathsf{AC}^0[p]$ for all primes p.

Theorem 18. *For all p prime,* $\mathsf{i\text{-}QAC}_2^0 \nsubseteq \mathsf{AC}^0[p]$.

Proof. From [37] and [2], we have that QNC_p^0 circuits can be implemented using single and two-qubit operations contained in $\mathsf{i\text{-}QNC}_2^0$. Furthermore, all quantum operations in QAC_p^0 used for the creation of the qudit-GHZ state in Lemmas 11 and 12 are controlled on a constant number of qudits and therefore these operations can be implemented $\mathsf{i\text{-}QNC}_2^0$.

Finally, we need to show that corrections needed to transform the poor man's cat states into qudit-GHZ states can be executed in $\mathsf{i\text{-}QAC}_2^0$. As described in the proof of Lemma 12, these corrections can be realized using a classical AC^0 circuit, which is encompassed by $\mathsf{i\text{-}QAC}_2^0$. Consequently, all quantum circuits from Theorems 13 and 17, for any prime p, can be constructed using $\mathsf{i\text{-}QAC}_2^0$ circuits. $\qquad\square$

2.5 Classical upper bounds for modular relation problems

In this subsection, we consider the classical upper bound on the modular relation problems, which indicates the limitations on the quantum/classical separations using our techniques.

Lemma 19. *For any fixed primes q,p and fixed $k_1, k_2, m \in \mathbb{N}$, $\mathcal{R}_{q^{k_1}, p^{k_2}}^m$ can be solved by an $\mathsf{NC}^0[p]$ circuit.*

Proof. We start by showing that there exists an $\mathsf{NC}^0[p]$ circuit that computes $\mathrm{MOD}_{p^{k_1}}$ for any $k_1 \in \mathbb{N}$. We use the $\mathsf{AC}^0[p]$ circuits described in [17] and argue that they can be implemented in $\mathsf{NC}^0[p]$.

We prove this statement by induction on the exponent k_1, showing that any MOD_{p^j} gate can be computed if we have access to $\mathrm{MOD}_{p^{j-1}}$ gates. The circuit construction from [17] is as follows:

1. For each $i \in [n]$, compute $y_i = \mathrm{MOD}_{p_{j-1}}(x)$.

2. For all $i \in 2, \ldots, n$, compute $z_i = \mathsf{AND}(y_{i-1}, \neg y_i)$.

3. Compute $b_j = \mathsf{AND}(\mathrm{MOD}_{p^{j-1}}(\sum_{i \in 2, \ldots, n} z_i), \mathrm{MOD}_p(|x|)) = \mathrm{MOD}_{p^j}(x)$.

Given that the final value $b_j = \mathrm{MOD}_{p^j}(x)$ [17], in order to show that MOD_{p^j} is in $\mathsf{NC}^0[p]$, we only need to show that each of these three steps can be implemented in $\mathsf{NC}^0[p]$. Let's evaluate these steps:

- The first step is inherently within $\mathsf{NC}^0[p]$ due to inductive reasoning; given the prior case produced an $\mathrm{MOD}_{p^{j-1}}$ gate, only the next steps need validation.

- The second step can be achieved with an NC^0 circuit since it solely relies on bounded fan-in AND gates.

- The third step follows since both modular gates are within $\mathsf{NC}^0[p]$ from our induction, combined with the AND gate having bounded fan-in.

Thus, any $\mathrm{MOD}_{p^{k_1}}$ gate can be implemented within $\mathsf{NC}^0[p]$ provided that k_1 is a constant, which determines the depth of the previously proposed circuit.

Finally, to prove our statement, i.e., to output a valid string for the modular relation problem $\mathcal{R}_{q^{k_1}, p^{k_2}}^m$, one needs to use the $\mathsf{NC}^0[p]$ circuit to compute the value of $\mathrm{MOD}_{p^{k_1}}(x)$ and then append it to a string like 0^{m-1}. We have that $|b_{k_1} 0^{m-1}| \pmod{q^{k_2}} = 0$ iff $|x| \pmod{p^{k_1}} = 0$. $\qquad\square$

Given the containment of the $\mathsf{NC}^0[p]$ circuit classes within the $\mathsf{AC}^0[p]$ classes, we have that all modular relation problems are solvable by TC^0 circuits.

Corollary 20. *For any primes q,p and $k_1, k_2, m \in \mathbb{N}$, $\mathcal{R}_{q^{k_1}, p^{k_2}}^m$ can be solved in TC^0.*

3 Shallow depth quantum circuits with infinite-size gate sets

This section considers constant-depth quantum circuits utilizing qubits and qudits, employing infinite gate sets and modular gates with unbounded fan-in while exploring their equivalences.

3.1 Constant-depth qudit circuits with quantum modular operators

In this subsection, we extend [42] and [29], and prove that the hierarchy of constant-depth quantum circuits with an infinite gateset over qudits collapses when we have access to a multi-qubit quantum/classical modular gate with unbounded fan-in gates.

We start by focusing on the quantum OR function, defined over Hilbert spaces of prime dimension p as follows,

$$\mathsf{qOR}\,|x_1, x_2, \ldots, x_n\rangle := |x_1 + \mathsf{OR}(x_2, x_3, \ldots, x_n) \pmod{p}, x_2, \ldots, x_n\rangle. \tag{33}$$

with the classical OR operating over strings in $\mathbb{F}_p$ defined as follows[6],

$$\mathsf{OR}(x) = \begin{cases} 1 & \text{if } \sum_{i=1}^n x_i > 0, \\ 0 & \text{otherwise.} \end{cases} \tag{34}$$

We first claim that a qudit analog of Høyer's and Špaleks OR reduction [22], which allows us to reduce the problem of computing qOR on an arbitrary state to the evaluation of qOR on another state with exponentially fewer qudits.

Lemma 21. *Let p be a prime. There exists a* $\mathsf{i\text{-}QNC}_p^0[p]$ *circuit C, such that for every n qudit state* $|\psi\rangle = \sum_{x \in \mathbb{F}_p^n} \alpha_x |x\rangle$, *we have*

$$C\,|\psi\rangle\,|0\rangle^{\otimes t} = \sum_{x \in \mathbb{F}_p^n,\ y \in \mathbb{F}_p^{\log_p(n)}} \alpha_x \beta_{y,x} |y\rangle |x\rangle |0\rangle^{\otimes t'} = |\psi^*\rangle |0\rangle^{\otimes t'}, \tag{35}$$

where and $\mathsf{qOR}\,|0\rangle\,|\psi\rangle = \mathsf{qOR}\,|0\rangle\,|\psi^*\rangle$ *with respect to the first qudit, while the second* qOR *does operate uniquely over the first $\log(n)$ qudits of $|\psi^*\rangle$.*

Proof. We describe now our circuit C. In the first step of this proposed circuit, we have a layer of n fanout gates, which are defined as follows

$$\mathsf{fanout}_p\,|x_1, x_2, \ldots, x_n\rangle := |x_1, (x_1 + x_2) \mod p, \ldots, (x_1 + x_n) \mod p\rangle. \tag{36}$$

The k-th fanout_p gate is applied to the k-th qudit of $|\psi\rangle$ and a fresh $\log_p(n)$-qudit state initialized on $|0\rangle^{\otimes \log(n)}$[7].

In parallel to these fanout_p gates, we create $\log_p(n)$ copies of n-qudit GHZ states. These can be created by an $\mathsf{QNC}_p^0[p]$ circuit using the method proposed in [33]. We have the following state

$$|\psi^{(1)}\rangle = C_{step\ 1}\,|\psi\rangle\,|0\rangle^{\otimes t} = \sum_{x \in \mathbb{F}_p^n} \alpha_x |x\rangle^{\otimes \log_p(n)} |\mathsf{GHZ}_{p,n}^0\rangle^{\otimes \log_p(n)} |0\rangle^{\otimes t'}. \tag{37}$$

For each $1 \leq k \leq \log_p(n)$, we apply n controlled rotations, where the j-th rotation of the k-th block will have as control the j-th qudit of the k-th copy of $|x\rangle$ and its target is the j-th qudit of the k-th GHZ state. The amplitude for all rotations in the k-th block is set to a fixed value of $\frac{2\pi}{p^k}$. Importantly, these operations can be implemented in constant depth due to the parallel copies of $|x\rangle$.

---

[6] The intuition behind the AND and OR functions over strings in $\mathbb{F}_p$ is that, similar to the binary case, the AND function discriminates against only one string, while the OR function includes all strings except one.

[7] Note that this fanout gate can be equally created from the qMOD_p gate, $\mathsf{fanout}_p = (\mathsf{F}_p)^{\otimes n}\mathsf{qMOD}_p(\mathsf{F}_p)^{\otimes n}$.

For a fixed x, this process modifies the k-th GHZ state to

$$\left(\bigotimes_{i=1}^{n} \mathsf{R}_Z^p\left(\frac{2\pi x_i}{p^k}\right)\right)|\mathsf{GHZ}_{p,n}^0\rangle = \sum_{x\in\mathbb{F}_p^n}\alpha_x\left(\frac{1}{\sqrt{p}}\sum_{j=0}^{p-1}e^{i\cdot\left(j\cdot\frac{2\pi}{p}\cdot\frac{|x|}{p^k}\right)}|j\rangle^{\otimes n}\right) \tag{38}$$

$$= \sum_{x\in\mathbb{F}_p^n}\alpha_x\sum_{j=0}^{p-1}c_{j,k,x}|\mathsf{GHZ}_{p,n}^j\rangle, \tag{39}$$

with $(c_{j,k,x})^2 = e^{i\left(j\left(\frac{2\pi}{p}\left(1-\frac{|x|}{p^k}\right)\right)\right)}$.

Note that for $|x| = 0$, all these GHZ states remain unchanged and are equal to $|\mathsf{GHZ}_{p,n}^0\rangle$. However, in contrast, we will now prove that for all basis states $|x\rangle$ with $|x| \geq 1$, one of the $\log_p(n)$ GHZ states we started with ends up in the form $|\mathsf{GHZ}_{p,n}^m\rangle$, where $m \neq 0$. In other words, for each nonzero x, there exists one value of k for which $c_{j,k,x}$ equals 1 for a single value of j and 0 for all others. Meanwhile, for the same value of x and all other values of k, $c_{j,k,x}$ takes non-unitary values for all values of j. To establish this, we utilize the fact that any integer number $|x|$ can always be decomposed as

$$|x| = p^{a_x}(p\cdot b_x + m_x), \tag{40}$$

with $a_x, b_x \in \mathbb{N}$ and $m_x \in [1, 2, \ldots, p-1]$. Hence, if $|x| > 0$, then we have that

$$\left(\bigotimes_{i=1}^{n}\mathsf{R}_Z^p\left(\frac{2\pi x_i}{p^{(a_x+1)}}\right)\right)|\mathsf{GHZ}_{p,n}^0\rangle = |\mathsf{GHZ}_{p,n}^{m_x}\rangle, \tag{41}$$

with $m_x \neq 0$ by definition. Therefore, $c_{j=m_x,k=a_x,x} = 1$ and $c_{j\neq m_x,k=a_x,x} = 0$, while for all the other GHZ states, these coefficients $c_{j,k\neq a_x,x}$ are non-unital as $\frac{2\pi}{p}(1-\frac{|x|}{p^k})$ is not a multiple of 2π. Thus, the state resulting from this set of controlled rotations is the following form,

$$|\psi^{(2)}\rangle = C_{step\ 2}\left(\sum_{x\in\mathbb{F}_p^n}\alpha_x|x\rangle^{\otimes\log_p(n)}|\mathsf{GHZ}_{p,n}^0\rangle^{\otimes\log_p(n)}\right)\otimes|0\rangle^{\otimes t'} \tag{42}$$

$$= \left(\alpha_{0^n}|0\rangle^{\otimes n\log_p(n)}|\mathsf{GHZ}_{p,n}^0\rangle_0|\mathsf{GHZ}_{p,n}^0\rangle_1\ldots|\mathsf{GHZ}_{p,n}^0\rangle_{\log_p(n)} + \sum_{x\in\mathbb{F}_p^n\setminus 0^n}\alpha_x|x\rangle^{\otimes\log_p(n)} \tag{43}$$

$$\ldots\left(\sum_{j=0}^{p-1}c_{j,a_x,x}|\mathsf{GHZ}_{p,n}^j\rangle\right)|\mathsf{GHZ}_{p,n}^{m_x}\rangle_{(a_x+1)}\left(\sum_{j=0}^{p-1}c_{j,(a_x+2),x}|\mathsf{GHZ}_{p,n}^j\rangle\right)\ldots\right)\otimes|0\rangle^{\otimes t'}. \tag{44}$$

We then apply Fourier gates $\mathsf{F}_p^{\otimes n}$ to the qudits initially entangled in GHZ states. Employing Lemma 8, we deduce that when $|x| = 0$, the resultant states form a superposition of strings with a Hamming weight congruent to zero modulo p. Conversely, for $|x| \geq 0$, at least one state transitions into a superposition of strings congruent modulo p to the inverse of m_x. It is important to note that since $m_x \bmod p$ is invariably non-zero, its additive inverse $-m_x \bmod p$ is likewise non-zero. Subsequently, we apply a qMOD_p gate with each of these states as control and as a target a new single qudit in a freshly initialized computational basis state $|0\rangle$ in our third register. The existence of the state described earlier ensures the qOR's intended effect, as at least one qudit in the third register will deterministically shift to a basis different from $|0\rangle$. For $|x| \geq 0$, since the GHZ states prior to the Fourier gates are superpositions in the Qudit-GHZ orthogonal X-basis, these strings after the Fourier gates are superpositions that align modulo p with potentially any value in $\mathbb{F}_p$. Consequently, in the third register, all other qudits assume superpositions dependent on the input, yet they do not influence the qOR operation.

Afterward, we apply a layer of the inverses of the Fourier gates $\mathsf{F}_p^{\otimes n}$ to exactly the same qudits in the second register as before, and consequently, they revert to the same states as described in Equations 43 and 44, being for all $k \in \{1, \ldots, \log(n)\}$ of the form

$$\sum_{x \in \mathbb{F}_p^n} \alpha_x \left(\frac{1}{\sqrt{p}} \sum_{j=0}^{p-1} e^{i \cdot \left(j \cdot \frac{2\pi}{p} \cdot \frac{|x|}{p^k} \right)} |j\rangle^{\otimes n} \right) = \sum_{x \in \mathbb{F}_p^n} \alpha_x \sum_{j=0}^{p-1} c_{j,k,x} |\mathsf{GHZ}_{p,n}^j\rangle . \tag{45}$$

This is possible because previously, we simply applied a qMOD_p with these states as control and did not change the target qudits. Thus, these states return to the same bases and states after the use of the inverse Fourier gates. Therefore, after these operations, we obtain the subsequent state, for which we do not represent the qudits of the third register in its position but next to each GHZ state that generated each one of them for a simpler representation.

$$C_{step\ 3} |\psi^{(2)}\rangle |0\rangle^{\otimes t'} = \left(\alpha_{0^n} |0\rangle^{\otimes (n \cdot \log_p(n))} |\mathsf{GHZ}_{p,n}^0\rangle_0 |\mathsf{GHZ}_{p,n}^0\rangle_1 \ldots |\mathsf{GHZ}_{p,n}^0\rangle_{\log_p(n)} |0\rangle^{\otimes \log_p(n)} \right. \tag{46}$$

$$+ \sum_{x \in \mathbb{F}_p^n \setminus 0^n} \alpha_x |x\rangle^{\otimes \log_p(n)} \ldots \left(\sum_{j=0}^{p-1} c_{j,a_x,x} |\mathsf{GHZ}_{p,n}^j\rangle |-j\rangle \right) |\mathsf{GHZ}_{p,n}^{m_x}\rangle_{(a_x+1)} |-m_x\rangle \tag{47}$$

$$\left. \left(\sum_{j=0}^{p-1} c_{j,(a_x+2),x} |\mathsf{GHZ}_{p,n}^j\rangle |-j\rangle \right) \ldots \right) \otimes |0\rangle^{\otimes t''} . \tag{48}$$

At this stage, all the qudits in the three registers are entangled. However, we can disentangle the first and third registers from the second, which contains the GHZ states. This disentanglement can be achieved using the third register that retains the phase information of the equivalent of the GHZ states, creating the entanglement between these two registers. For that, we use generalized controlled rotations, with the control based on the qudits of the third register, applied to one qudit of the respective GHZ state of amplitude $\frac{2\pi}{p^k}$. For simplicity, we will consider first the effect on a single basis of $|x\rangle$,

$$\alpha_x |x\rangle^{\otimes \log_p(n)} \ldots \left(\sum_{j=0}^{p-1} c_{j,a_x,x} \left(\mathsf{CGR}\left(\frac{2\pi}{p^k} \right) |\mathsf{GHZ}_{p,n}^j\rangle |-j\rangle \right) \right) \ldots \tag{49}$$

$$= \alpha_x |x\rangle^{\otimes \log_p(n)} \ldots \left(\frac{1}{\sqrt{p}} \sum_{j=0}^{p-1} e^{i \cdot \left(j \cdot \frac{2\pi}{p} \cdot \frac{|x|}{p^k} \right)} \left(\mathsf{CGR}\left(\frac{2\pi}{p^k} \right) |j\rangle^{\otimes n} |-j\rangle \right) \right) \ldots \tag{50}$$

$$= \alpha_x |x\rangle^{\otimes \log_p(n)} \ldots \left(\frac{1}{\sqrt{p}} \sum_{j=0}^{p-1} e^{i \cdot \left(j \cdot \frac{2\pi}{p} \cdot \frac{|x|}{p^k} \right)} e^{i \cdot \left(-j \cdot \frac{2\pi}{p} \cdot \frac{|x|}{p^k} \right)} |j\rangle^{\otimes n} |-j\rangle \right) \ldots \tag{51}$$

$$= \alpha_x |x\rangle^{\otimes \log_p(n)} \ldots \left(\sum_{j=0}^{p-1} |\mathsf{GHZ}_{p,n}^0\rangle |-j\rangle \right) \ldots . \tag{52}$$

Now as the previous transformation is independent of the respective basis $|x\rangle$, we obtain the fol-

lowing state,

$$C_{step\ 4} |\psi^{(3)}\rangle |0\rangle^{\otimes t''} = \left(\alpha_{0^n} |0\rangle^{\otimes(n\cdot\log_p(n))} |\mathsf{GHZ}^0_{p,n}\rangle_0 |\mathsf{GHZ}^0_{p,n}\rangle_1 \dots |\mathsf{GHZ}^0_{p,n}\rangle_{\log_p(n)} |0\rangle^{\otimes\log_p(n)} \right. \quad (53)$$

$$+ \sum_{x\in\mathbb{F}_p^n\backslash 0^n} \alpha_x |x\rangle^{\otimes\log_p(n)} \dots |\mathsf{GHZ}^0_{p,n}\rangle \left(\sum_{j=0}^{p-1} c_{j,a_x,x} |-j\rangle \right) |\mathsf{GHZ}^0_{p,n}\rangle_{(a_x+1)} |-m_x\rangle \quad (54)$$

$$\left. |\mathsf{GHZ}^0_{p,n}\rangle \left(\sum_{j=0}^{p-1} c_{j,(a_x+2),x} |-j\rangle \right) \dots \right) \otimes |0\rangle^{\otimes t''}. \quad (55)$$

Consequently, we end up with $\log_p(n)$ GHZ states of the form $|\mathsf{GHZ}^0_{p,n}\rangle$, which are no longer entangled with the other registers, as intended. These states and the repetitions of the initial state can be easily removed using the fanout gates and their inverses[8] obtaining the following state,

$$|\psi^{(5)}\rangle = C_{step\ 5} |\psi^{(4)}\rangle = \left(\alpha_{0^n} |0\rangle^{\otimes(n+\log_p(n))} + \sum_{x\in\mathbb{F}_p^n\backslash 0^n} \alpha_x |x\rangle \dots \left(\sum_{j=0}^{p-1} c_{j,a_x,x} |-j\rangle \right) |-m_x\rangle \quad (56)$$

$$\left(\sum_{j=0}^{p-1} c_{j,(a_x+2),x} |-j\rangle \right) \dots \right) \otimes |0\rangle^{\otimes t'''} = \sum_{x\in\mathbb{F}_p^n,\ y\in\mathbb{F}_p^{\log_p(n)}} \alpha_x\beta_{y,x} |x\rangle |y\rangle \otimes |0\rangle^{\otimes t'''}. \quad (57)$$

Finally, if we take $|\psi^*\rangle$ as $|\psi^5\rangle$ with the first and second register swapped, we obtain that the former state satisfies the property $\mathsf{qOR}\,|0\rangle\,|\psi\rangle = \mathsf{qOR}\,|0\rangle\,|\psi^*\rangle$ on the first qudit, with the second qOR applied only to the first $\log(n)$ qudits. This is justified by that fact that the basis $|0\rangle^{\otimes\log_p(n)}$ in $|\psi^*\rangle$ has the same amplitude as the basis $|0\rangle^{\otimes n}$ in $|\psi\rangle$. The same principle forcefully applies to set all the bases orthogonal to the previously described, as demonstrated in Equations 56 and 57. Therefore, the effect of the qOR function on the first qudit state is equal for both cases considered completing the proof. $\qquad\square$

The second step shows an exponential-size i-QNC_p^0 circuit for qOR. For that, we use the following theorem on the representation of functions as a multi-linear polynomial over $\mathbb{F}_p$, expanding previous uses of these objects over $\mathbb{F}_2$ and $\mathbb{F}_3$ [29, 31, 27].

Theorem 22. *[26] Every function $f: \mathbb{F}_p^n \to \mathbb{R}$ can be expressed as a polynomial*

$$f(x) = \sum_{k_1,k_2,\dots,k_n\in\mathbb{F}_p} \widehat{f}(\chi_{k_1,k_2,\dots,k_n}) \cdot \chi_{k_1,k_2,\dots,k_n}(x), \quad (58)$$

with $\widehat{f}(\chi_{k_1,k_2,\dots,k_n})$ being a real coefficient, and $\chi_{k_1,k_2,\dots,k_n}(x)$ multi-linear function in $\mathbb{F}_p$.

We now extend the techniques of [42] to show that our exponential-size circuit for qOR.

Lemma 23. *For any prime p, qOR can be implemented on an n-qudit state using $\mathcal{O}(n \cdot p^n)$ operations in i-$\mathsf{QNC}_p^0[p]$.*

Proof. Let us describe the i-QNC_p^0 circuit that computes qOR. The first layer of the circuit consists of $n-1$ fanout gates, where the i-th gate is controlled by the $(i+1)$-th qudit of the initial state to a new register initialized to $|0\rangle^{\otimes p^{n-1}}$. This maps the initial state $|0\rangle |\psi\rangle |0\rangle^{\otimes t}$ to

$$|0\rangle \sum_{x\in\mathbb{F}_p^{n-1}} \alpha_x |x\rangle \left(|x_2,\dots,x_n\rangle \right)^{\otimes p^{n-1}} |0\rangle^{\otimes t'}. \quad (59)$$

---

[8] The inverse of the fanout_p gate is simply $(\mathsf{fanout}_p)^{p-1}$.

We then apply p^{n-1} parallel qMOD_p gates, where the i-th gate is applied on the i-th block of the previous state, and the qMOD_p computes a different $\chi_{k_1, k_2, \ldots, k_n}$ leading to

$$|0\rangle \sum_{x \in \mathbb{F}_p^n} \alpha_x |x\rangle \left(\bigotimes_{k_1, \ldots, k_{n-1} \in \mathbb{F}_p} |x_2, \ldots, x_n\rangle |\chi_{k_1, k_2, \ldots, k_{n-1}}(x_2, \ldots, x_n)\rangle \right) |0\rangle^{\otimes t'}. \tag{60}$$

We then create a $|\mathsf{GHZ}_{p, p^{n-1}}^0\rangle$ state and we apply generalized controlled rotations as follows. The i-th rotation has as control the register where $\chi_{k_1, k_2, \ldots, k_n}(x_2, \ldots, x_n)$ is computed and the target is the i-th qudit of the GHZ state. The angle of the rotation is $\widehat{f_{\overline{\mathsf{OR}}}}(\chi_{k_1, k_2, \ldots, k_n})$. These angles are defined by the $\overline{\mathsf{OR}}$ function which is defined as follows,

$$\overline{\mathsf{OR}}(x) = \begin{cases} p - 1 & \text{if } \sum_{i=1}^n x_i > 0, \\ 0 & \text{otherwise.} \end{cases} \tag{61}$$

and that we decompose, according to Theorem 22 as

$$\overline{\mathsf{OR}}(x) = \sum_{k_1, k_2, \ldots, k_n \in \mathbb{F}_p} \widehat{f_{\overline{\mathsf{OR}}}}(\chi_{k_1, k_2, \ldots, k_n}) \cdot \chi_{k_1, k_2, \ldots, k_n}(x) \tag{62}$$

to obtain the following state on this last register,

$$|\overline{\mathsf{OR}}\rangle = \sum_{x \in \mathbb{F}_p^n} \alpha_x \left(\frac{1}{\sqrt{p}} \sum_{j=0}^{p-1} e^{j \cdot \frac{\pi}{p} \left(\sum_{k_1, k_2, \ldots, k_{n-1} \in \mathbb{F}_p} \widehat{f_{\overline{\mathsf{OR}}}}(\chi_{k_1, k_2, \ldots, k_{n-1}}) \cdot \chi_{k_1, k_2, \ldots, k_{n-1}}(x_2 \ldots x_n) \right)} |j\rangle^{\otimes p^{n-1}} \right)$$

$$= \sum_{x \in \mathbb{F}_p^n} \alpha_x \left(\frac{1}{\sqrt{p}} \sum_{j=0}^{p-1} e^{\frac{j \cdot \pi \cdot \overline{\mathsf{OR}}(x_2 \ldots x_n)}{p}} |j\rangle^{\otimes p^{n-1}} \right) = \sum_{x \in \mathbb{F}_p^n} \alpha_x |\mathsf{GHZ}_{p, p^{n-1}}^{\overline{\mathsf{OR}}(x_2, \ldots, x_n)}\rangle.$$

In the last step, we apply the Fourier gate to all the qudits in the newly created state in the third register and a single use of the quantum modular gate qMOD_p from all the qudits to the first qudit in the state $|0\rangle$. Using Lemmas 7 and 8, we obtain the state

$$\sum_{x \in \mathbb{F}_p^n} \alpha_x |\overline{\mathsf{OR}}(x_2 \ldots x_n)^{-1}\rangle |x_1, x_2, \ldots, x_n\rangle$$

$$\left(\bigotimes_{k_1, \ldots, k_{n-1}} |x_2, \ldots, x_n\rangle |\chi_{k_1, k_2, \ldots, k_{n-1}}(x_2, \ldots, x_n)\rangle \right) \left(\frac{1}{\sqrt{p^{n-2}}} \sum_{\substack{z \in \mathbb{F}_p^{n-1} \\ |z| \mod p = -\overline{\mathsf{OR}}(x_2, \ldots, x_n)}} |z\rangle \right).$$

Next, we apply a SUM gate to the first qudit, with the first qudit from the initial state $|\psi\rangle$. This ensures we obtain the expected output state from applying qOR function on the input state $|\psi\rangle$ given that $-\overline{\mathsf{OR}}(x_2, \ldots, x_n) = \mathsf{OR}(x_2, \ldots, x_n)$. Finally, we execute the inverse operations on the auxiliary qudits to decouple these from the input state. We can do this because all operations acting on the input state and auxiliary qudits are unitary. In addition, the inverse operations of fanout_p, qMod_p, and of the controlled rotations—are all within $\mathsf{QNC}_p^0[p]$. See Appendix A.2.1 for details on the first two operations. $\qquad \square$

We now prove our first collapse of the different classes on constant-depth quantum circuits.

Theorem 24. $\mathsf{i\text{-}QNC}_p[p] = \mathsf{i\text{-}QAC}_p[p]$, *for any p prime.*

Proof. To prove this collapse, we need only to show that qOR and the qAND operation can be implemented by an i-QNC$_p$[p] circuit. The latter gate is already the Toffoli X gate, which we can use to obtain any other multi-qudit Toffoli gate.

To implement qOR, we integrate circuits C_1 and C_2 from Lemmas 21 and 23, respectively. Circuit C_1 effectively reduces the number of qudits in the state $|\psi\rangle$, generating a new state $|\psi^*\rangle$ that preserves the qOR output alongside a fresh $|0\rangle$, and C_2 performs the actual qOR computation. By applying C_1 to all qudits of $|\psi\rangle$ except the first, and subsequently feeding $|0\rangle |\psi^*\rangle$ to C_2. The global output is generated by applying the SUM gate to the first qudit $\sum_{x\in[p^{n-1}]} \alpha_{x_2,...,x_n} |OR(x_2,...,x_n)\rangle$ resulting from C_2 and the first qudit of the initial $|\psi\rangle$ state.

To conclude the proof, we return all auxiliary qudits to their initial state, $|0\rangle^{\otimes t}$. Initially, we observe that $\log(n)$ auxiliary qudits arise from the OR reduction. We then apply the exponentially large qOR operator, described in Lemma 23, to these $\log_p(n)$ qudits. Importantly, this step does not introduce additional auxiliary qudits. Thus, our goal now is to reverse the state of these $\log(n)$ auxiliary qudits to $|0\rangle^{\otimes \log_p(n)}$, without impacting the result obtained from the qOR operation. We notice that undoing the operation on the $\log(n)$ qubits is possible since the operations of Lemma 21 can be reverted even if the first and second registers are entangled with the qubit where the qOR was applied. This implies that the $\log(n)$ qudits were unnecessary to achieve the intended final state. Hence, we can reversibly return these qudits to their initial state without losing any information.

The reversal process is straightforward. We follow the steps used to generate these $\log_p(n)$ qudits but omit the application of the qMOD operator, as delineated in Lemma 21. Instead, we employ the qMOD^{p-1} operator. This ensures that all qudits are restored to the $|0\rangle$ state, completing the process unitarily. □

For the next collapse, we need to demonstrate that the quantum threshold gate is in i-QNC$_p^0$[p]. For that, we first demonstrate that the quantum version of the Exact$_k$ function is contained in the same circuit class.

Definition 25. Exact$_k$. *The* Exact$_k$ *function is defined as follows,*

$$\text{Exact}_k(x) = \begin{cases} 1 & \text{if } \sum_{i=1}^n x_i = k \\ 0 & \text{otherwise} \end{cases}, \tag{63}$$

and its quantum analog as the following operation over Hilbert spaces of prime dimension p

$$\text{qExact}_k |x_1, x_2, \ldots, x_n\rangle := |x_1 + \text{Exact}_k(x_2, x_3, \ldots, x_n) \pmod p, x_2, \ldots, x_n\rangle. \tag{64}$$

Lemma 26. *For any prime p,* qExact *can be implemented in* i-QNC$_p^0$[p].

Proof. We approach this problem once again using a constructive method, retaining most elements from the circuit used for the qOR function. The qOR function fundamentally discerns whether a computational basis state has a Hamming weight of zero. However, the initial step involving the qOR reduction will be modified. Previously, this reduction applied controlled rotations to GHZ states, effectively implementing a rotation with an amplitude proportional to the Hamming weight of the computational basis states, denoted as $\frac{2\pi|x|}{p^i}$. The new circuit introduces additional rotations to each i-th GHZ state with an amplitude of $-\frac{2\pi k}{p^i}$ respectively. This supplemental rotation emulates the behavior of the original circuit, equating the effects of a string with a Hamming weight of zero to those of a string with a Hamming weight of k. As a result, when these modified states are subsequently processed by the remaining qOR circuitry, the outcome will precisely compute the qExact$_k$ function. □

Using Lemma 26, we push the collapse of Theorem 24 further to constant-depth quantum circuits with threshold gates.

Theorem 27. *For any prime p,* i-QNC$_p$[p] = i-QTC$_p$.

Proof. To prove this statement, it is sufficient to show that qTH_k can be implemented in i-$\mathsf{QNC}_p[p]$. The circuit for qTH_k is composed of $n - k$ qExact_t operations (described in Lemma 26) for which t will range from k to n. In this setup, the fanout gate is employed to parallelize the application of the qExact_t operations. As a result, we generate states of the form $\sum_{x \in \mathbb{F}_p^{n-1}} \alpha_x |\mathsf{Exact}_k(x_2 \ldots x_n)\rangle |x\rangle$ based on the input state $|\psi\rangle = \sum_{x \in \mathbb{F}_p^n} \alpha_x |0\rangle^{\otimes(n-k)} |x\rangle$.

Subsequently, the qOR gate will be applied to all these states, and a computational basis state $|0\rangle$, obtained with the following state,

$$\sum_{x \in \mathbb{F}_p^n} \alpha_x |\mathsf{OR}(\mathsf{Exact}_k(x_2 \ldots x_n), \mathsf{Exact}_{k+1}(x_2 \ldots x_n), \ldots, \mathsf{Exact}_n(x_2 \ldots x_n))\rangle \tag{65}$$

$$|\mathsf{Exact}_k(x_2 \ldots x_n)\rangle_k \ldots |\mathsf{Exact}_k(x_2 \ldots x_n)\rangle_n |x\rangle^{\otimes(n-k)} \tag{66}$$

$$= \sum_{x \in \mathbb{F}_p^n} \alpha_x |\mathsf{TH}_k(x_1 \ldots x_n)\rangle \ldots |x\rangle^{\otimes(n-k)} \ . \tag{67}$$

It requires only applying the SUM gate between the first qudit and the first qudit of the state $|\psi\rangle$, and we obtain the state resulting from applying the qTH_k on the input state $|\psi\rangle$. The last step resumes applying all the inverse unitaries on the auxiliary qudits to detangle those from the resulting state. Lastly, we apply the inverse unitaries to all auxiliary qudits, disentangling them from the final state while preserving the desired output. $\qquad\square$

3.2 Constant-depth qudit circuits with classical modular operators

In this section, we consider the collapse of constant-depth circuits with infinite-size quantum gate sets and classical modular gates.

We first show that quantum modular gates can be implemented with constant depth measurement patterns and classical modular gates.

Lemma 28. *The* qMOD_p *gate can be implemented in* i-$\mathsf{QNC}_p^0[p]_\mathsf{c}$.

Proof. Our first step in this proof is to show that a circuit in i-$\mathsf{QNC}_p^0[p]_\mathsf{c}$ can implement the fanout_p gate over an arbitrary quantum state, $|\psi\rangle = \sum_{x \in \{0,1,\ldots,p-1\}^n} \alpha_x |x\rangle$.

For that, we first create an $|\mathsf{GHZ}_{p,n}^0\rangle$ state and apply a SUM where the control-qudit is the first qudit of $|\psi\rangle$ and the target is the first qudit of the GHZ state. This leads to the state,

$$|\psi^{(1)}\rangle = \sum_{x \in \mathbb{F}_p^n} \alpha_x (\mathsf{I}^{\otimes n} \otimes (\mathsf{X}_p)^{x_1} \otimes \mathsf{I}^{\otimes(n-1)}) |x\rangle |\mathsf{GHZ}_p^0\rangle \ . \tag{68}$$

Subsequently, we measure the first qudit of the second register with outcome $m_1 \in \{0, 1, \ldots, p-1\}$. The post-measured state will then be

$$|\psi^{(2)}\rangle = \sum_{x \in \mathbb{F}_p^n} \alpha_x |x_1, x_2 \ldots x_n, m_1, (x_1 + m_1) \mod p, \ldots, (x_1 + m_1) \mod p\rangle \ . \tag{69}$$

We then apply $(\mathsf{X}_p)^{-m_1}$ to each of the $n - 1$ qudits of the second register, leading to the state

$$|\psi^{(3)}\rangle = \sum_{x \in \mathbb{F}_p^n} \alpha_x |x_1, x_2, \ldots, x_n, m_1, x_1, \ldots, x_1\rangle \ . \tag{70}$$

Using this state, we can apply a layer of $n - 1$ parallel SUM gates where the control gate is one of the $n - 1$ last qudits, and the target is one of the qudits from the 2nd to the n-th qudit in the first register. Resulting in the following state

$$|\psi^{(4)}\rangle = \sum_{x \in \mathbb{F}_p^n} \alpha_x |x_1, (x_2 + x_1) \mod p, \ldots, (x_n + x_1) \mod p, m_1, x_1, \ldots, x_1\rangle \ , \tag{71}$$

which is equivalent to applying the fanout_p gate on state $|\psi^{(3)}\rangle$.

The last step is to remove the entanglement between the first n qudits and the last $n-1$ ones. For that, we apply the Fourier gate to the last $n-1$ qudits, and we have

$$|\psi^{(5)}\rangle = \frac{1}{\sqrt{p^n}} \sum_{m_2...m_n \in \mathbb{F}_p^{n-1}} \sum_{x \in \mathbb{F}_p^n} \alpha_x \cdot e^{i\frac{-2\pi x_1(\sum_{i=2}^n m_i)}{p}} \tag{72}$$

$$|x_1, (x_2 + x_1) \bmod p, \ldots, (x_{n-1} + x_1) \bmod p, m_1, \ldots, m_n\rangle \ . \tag{73}$$

We can then measure the last $n-1$ qudits with outcome $m_2, ..., m_n \in \mathbb{F}_p$ to determine the value of $\phi = -\sum_{i=2}^n m_i \pmod p$ and apply a controlled generalized rotation CGR_Z^p with control on x_1 and parameterized by ϕ to remove the relative phase introduced by the Fourier gates[9]. Tracing out the measured states, we have the state

$$|\psi^{(6)}\rangle = \sum_{x \in \mathbb{F}_p^n} \alpha_x |x_1, (x_2 + x_1) \bmod p, \ldots, (x_n + x_1) \bmod p\rangle \ . \tag{74}$$

which corresponds to state $(\mathsf{fanout_p} |\psi\rangle)$, as intended.

Finally, we only need to use the circuit that translates the fanout_p gate to the qMOD_p gate, using simply the standard translation presented by qubits [22] in higher dimensions with the Fourier gates. This and the fact that all the sub-processes described previously are contained in $\mathsf{i}\text{-}\mathsf{QNC}_p^0[p]_{\mathsf{c}}$ completes the proof. □

Using this lemma and the results in the previous subsection we can prove the following.

Lemma 29. *For any prime p, $\mathsf{i}\text{-}\mathsf{QNC}_p[p]_{\mathsf{c}} = \mathsf{i}\text{-}\mathsf{QTC}_p$.*

Proof. It follows from Lemma 28 that $\mathsf{i}\text{-}\mathsf{QNC}_p[p]_{\mathsf{c}} = \mathsf{i}\text{-}\mathsf{QNC}_p^0[p]$. The result follows since $\mathsf{i}\text{-}\mathsf{QTC}_p = \mathsf{i}\text{-}\mathsf{QNC}_p^0[p]$ from Theorem 27. □

Lemma 29 shows that the implementation of constant-depth MBQC over prime dimensional qudits is capable of the same type of circuit collapses as all the ones that have been demonstrated for qubits. Now we show how these circuit classes compare to each other.

Theorem 30. *For any p and q prime. $\mathsf{i}\text{-}\mathsf{QTC}_p^0 \subseteq \mathsf{i}\text{-}\mathsf{QNC}_2^0[q]_{\mathsf{c}}$.*

Proof. The proof proceeds in two steps. Firstly, we show that $\mathsf{i}\text{-}\mathsf{QNC}_q^0$ and $\mathsf{i}\text{-}\mathsf{QNC}_p^0$ are contained in $\mathsf{i}\text{-}\mathsf{QNC}_2^0$ for any primes p and q. To establish this, we need a mapping from the qudit basis to the qubit basis for both prime dimensions, p and q. For example, qutrits can be mapped to qubits using the following correspondence: $|0\rangle \to |00\rangle$, $|1\rangle \to |01\rangle$ and $|2\rangle \to |11\rangle$, utilizing only a subspace of the Hilbert space of dimension 4. Consequently, any qudit can be translated into $2\lceil p/2\rceil$ qubits. Additionally, any unitary operator over a Hilbert space of dimensions p and $2p$ can be mapped to a unitary operator over a Hilbert space of dimensions $2\lceil p/2\rceil$ and $4\lceil p/2\rceil$. This new operator applies the same transformation over the encoded qubit basis as the original did over the qudits, while the basis ignored by the encoding is operated by the identity locally.

This argument can be augmented with the demonstration that all such fixed sizes can be constructed in constant depth using single and two-qubit gates, as described in [37] and [2]. These methods prove that any unitary operator on k qubits can be synthesized using at most $\mathcal{O}(k^3 4^k)$ two-qubit gates. This further suggests that all operations in $\mathsf{i}\text{-}\mathsf{QNC}_q^0$ and $\mathsf{i}\text{-}\mathsf{QNC}_p^0$ can be executed by an $\mathsf{i}\text{-}\mathsf{QNC}_2^0$ circuit with a specific encoding for each prime dimension.

Given that all operations in $\mathsf{i}\text{-}\mathsf{QNC}_q^0$ can be achieved within $\mathsf{i}\text{-}\mathsf{QNC}_2^0$, it follows that all operations in $\mathsf{i}\text{-}\mathsf{QNC}_q^0[q]_{\mathsf{c}}$ also belong to $\mathsf{i}\text{-}\mathsf{QNC}_2^0[q]_{\mathsf{c}}$. This implies that $\mathsf{i}\text{-}\mathsf{QNC}_2^0[q]_{\mathsf{c}}$ contains the MOD_p gate.

---

[9]The value of ϕ is classical and can be determined using the classical MOD_p gates with a binary outcome in the form of p bits, with only one of them being equal to 1, determining the value ϕ.

Coupled with the fact that i-QNC_2^0 can implement all the operations in i-QNC_p^0, we deduce that i-$\mathsf{QNC}_2^0[q]_{\mathsf{c}}$ can execute all operations in i-$\mathsf{QNC}_p^0[p]_{\mathsf{c}}$ for any given prime p. The final piece to consider is Lemma 29, which allows us to arrive at the desired result. $\square$

Building on this result, we can also extend the quantum-classical separations illustrated by [18] and [42], which separated i-$\mathsf{QNC}_2^0[2]$ from the classical $\mathsf{AC}^0[p]$ classes.

Corollary 31. *For all p and q prime,* i-$\mathsf{QNC}_2^0[q]_{\mathsf{c}} \nsubseteq \mathsf{AC}^0[p]$.

Proof. The i-$\mathsf{QNC}_2^0[q]_{\mathsf{c}}$ class contains all the operations of i-QNC_q^0; therefore, it contains all the operations in i-QTC_q^0, which include all the MOD_k operations, with k prime. This is combined with Razborov-Smolensky separations (Theorem 35), which states that all $\mathsf{AC}^0[p]$ classes fail to compute any MOD_k gate other than the MOD_p gate with p and k being two distinct prime numbers finishes the proof. $\square$

References

[1] Sanjeev Arora and Boaz Barak. *Computational complexity: a modern approach.* Cambridge University Press, 2009.

[2] Adriano Barenco, Charles H. Bennett, Richard Cleve, David P. DiVincenzo, Norman Margolus, Peter Shor, Tycho Sleator, John A. Smolin, and Harald Weinfurter. Elementary gates for quantum computation. *Phys. Rev. A*, 52:3457–3467, Nov 1995.

[3] Adam Bene Watts and Natalie Parham. Unconditional Quantum Advantage for Sampling with Shallow Circuits. *arXiv e-prints*, page arXiv:2301.00995, January 2023.

[4] Debajyoti Bera. A lower bound method for quantum circuits. *Information processing letters*, 111(15):723–726, 2011.

[5] Robert Ivan Booth. *Measurement-based quantum computation beyond qubits.* Theses, Sorbonne Université, February 2022.

[6] Sergey Bravyi, David Gosset, and Robert König. Quantum advantage with shallow circuits. *Science*, 362(6412):308–311, 2018.

[7] Sergey Bravyi, Isaac Kim, Alexander Kliesch, and Robert Koenig. Adaptive constant-depth circuits for manipulating non-abelian anyons. *arXiv preprint arXiv:2205.01933*, 2022.

[8] Sergey Bravyi, Dmitri Maslov, and Yunseong Nam. Constant-cost implementations of clifford operations and multiply-controlled gates using global interactions. *Physical Review Letters*, 129(23):230501, 2022.

[9] Jop Briët, Harry Buhrman, Davi Castro-Silva, and Niels MP Neumann. Noisy decoding by shallow circuits with parities: classical and quantum. *arXiv preprint arXiv:2302.02870*, 2023.

[10] Dan Browne, Elham Kashefi, and Simon Perdrix. Computational depth complexity of measurement-based quantum computation. In Wim van Dam, Vivien M. Kendon, and Simone Severini, editors, *Theory of Quantum Computation, Communication, and Cryptography*, pages 35–46, Berlin, Heidelberg, 2011. Springer Berlin Heidelberg.

[11] Dan Browne, Elham Kashefi, and Simon Perdrix. Computational depth complexity of measurement-based quantum computation. In Wim van Dam, Vivien M. Kendon, and Simone Severini, editors, *Theory of Quantum Computation, Communication, and Cryptography*, pages 35–46, Berlin, Heidelberg, 2011. Springer Berlin Heidelberg.

[12] Daniel E Browne, Elham Kashefi, Mehdi Mhalla, and Simon Perdrix. Generalized flow and determinism in measurement-based quantum computation. *New Journal of Physics*, 9(8):250, aug 2007.

[13] Matthew Coudron, Jalex Stark, and Thomas Vidick. Trading locality for time: certifiable randomness from low-depth circuits. *Communications in mathematical physics*, 382:49–86, 2021.

[14] M. Fang, S. Fenner, F. Green, S. Homer, and Y. Zhang. Quantum lower bounds for fanout. *Quantum Info. Comput.*, 6(1):46–57, jan 2006.

[15] Merrick Furst, James B Saxe, and Michael Sipser. Parity, circuits, and the polynomial-time hierarchy. *Mathematical systems theory*, 17(1):13–27, 1984.

[16] Oded Goldreich. Three xor-lemmas—an exposition. *Studies in Complexity and Cryptography. Miscellanea on the Interplay between Randomness and Computation: In Collaboration with Lidor Avigad, Mihir Bellare, Zvika Brakerski, Shafi Goldwasser, Shai Halevi, Tali Kaufman, Leonid Levin, Noam Nisan, Dana Ron, Madhu Sudan, Luca Trevisan, Salil Vadhan, Avi Wigderson, David Zuckerman*, pages 248–272, 2011.

[17] Oded Goldreich. On teaching the approximation method for circuit lower bounds. *Eletronical Colloquium on Computational Complexity*, 2023.

[18] Frederic Green, Steven Homer, Cristopher Moore, and Christopher Pollett. Counting, fanout and the complexity of quantum acc. *Quantum Info. Comput.*, 2(1):35–65, dec 2002.

[19] Daniel Grier and Luke Schaeffer. Interactive shallow clifford circuits: Quantum advantage against nc¹ and beyond. In *Proceedings of the 52nd Annual ACM SIGACT Symposium on Theory of Computing*, STOC 2020, page 875–888, New York, NY, USA, 2020. Association for Computing Machinery.

[20] Koen Groenland, Freek Witteveen, Kareljan Schoutens, and Rene Gerritsma. Signal processing techniques for efficient compilation of controlled rotations in trapped ions. *New Journal of Physics*, 22(6):063006, 2020.

[21] Nikodem Grzesiak, Andrii Maksymov, Pradeep Niroula, and Yunseong Nam. Efficient quantum programming using ease gates on a trapped-ion quantum computer. *Quantum*, 6:634, 2022.

[22] Peter Høyer and Robert Špalek. Quantum fan-out is powerful. *Theory of Computing*, 1(5):81–103, 2005.

[23] Yanglin Hu, Darya Melnyk, Yuyi Wang, and Roger Wattenhofer. Space complexity of streaming algorithms on universal quantum computers. In *Theory and Applications of Models of Computation: 16th International Conference, TAMC 2020, Changsha, China, October 18–20, 2020, Proceedings 16*, pages 275–286. Springer, 2020.

[24] Richard Jozsa. An introduction to measurement based quantum computation. *NATO Science Series, III: Computer and Systems Sciences. Quantum Information Processing-From Theory to Experiment*, 199:137–158, 2006.

[25] Zhenning Liu and Alexandru Gheorghiu. Depth-efficient proofs of quantumness. *Quantum*, 6:807, September 2022.

[26] Bao Luong. *Fourier analysis on finite Abelian groups*. Springer Science & Business Media, 2009.

[27] Jelena Mackeprang, Daniel Bhatti, Matty J Hoban, and Stefanie Barz. The power of qutrits for non-adaptive measurement-based quantum computing. *New Journal of Physics*, 25(7):073007, jul 2023.

[28] Dmitri Maslov and Yunseong Nam. Use of global interactions in efficient quantum circuit constructions. *New Journal of Physics*, 20(3):033018, 2018.

[29] Ryuhei Mori. Periodic fourier representation of boolean functions. *arXiv preprint arXiv:1803.09947*, 2018.

[30] Shivam Nadimpalli, Natalie Parham, Francisca Vasconcelos, and Henry Yuen. On the Pauli Spectrum of QAC0. *arXiv e-prints*, page arXiv:2311.09631, November 2023.

[31] Michael de Oliveira, Luís S. Barbosa, and Ernesto F. Galvão. Quantum advantage in temporally flat measurement-based quantum computation. *Quantum*, 8:1312, April 2024.

[32] Daniel Padé, Stephen Fenner, Daniel Grier, and Thomas Thierauf. Depth-2 qac circuits cannot simulate quantum parity. *arXiv preprint arXiv:2005.12169*, 2020.

[33] Filipa C. R. Peres. The Pauli-based model of quantum computation with higher dimensional systems. *arXiv e-prints*, page arXiv:2302.13702, February 2023.

[34] John Preskill. Quantum Computing in the NISQ era and beyond. *Quantum*, 2:79, August 2018.

[35] Robert Raussendorf and Hans J. Briegel. A one-way quantum computer. *Phys. Rev. Lett.*, 86:5188–5191, May 2001.

[36] Robert Raussendorf and Hans J. Briegel. Computational model underlying the one-way quantum computer. *Quantum Info. Comput.*, 2(6):443–486, oct 2002.

[37] Michael Reck, Anton Zeilinger, Herbert J. Bernstein, and Philip Bertani. Experimental realization of any discrete unitary operator. *Phys. Rev. Lett.*, 73:58–61, Jul 1994.

[38] Gregory Rosenthal. Bounds on the qac^0 complexity of approximating parity. *arXiv preprint arXiv:2008.07470*, 2020.

[39] Benjamin Rossman, Rocco A. Servedio, and Li-Yang Tan. Complexity theory column 89: The polynomial hierarchy, random oracles, and boolean circuits. *SIGACT News*, 46(4):50–68, dec 2015.

[40] Atul Singh Arora, Andrea Coladangelo, Matthew Coudron, Alexandru Gheorghiu, Uttam Singh, and Hendrik Waldner. Quantum Depth in the Random Oracle Model. *arXiv e-prints*, page arXiv:2210.06454, October 2022.

[41] R. Smolensky. Algebraic methods in the theory of lower bounds for boolean circuit complexity. In *Proceedings of the Nineteenth Annual ACM Symposium on Theory of Computing*, STOC '87, page 77–82, New York, NY, USA, 1987. Association for Computing Machinery.

[42] Yasuhiro Takahashi and Seiichiro Tani. Collapse of the hierarchy of constant-depth exact quantum circuits. *computational complexity*, 25:849–881, 2016.

[43] Maarten Van den Nest, Akimasa Miyake, Wolfgang Dür, and Hans J. Briegel. Universal resources for measurement-based quantum computation. *Phys. Rev. Lett.*, 97:150504, Oct 2006.

[44] Adam Bene Watts, Robin Kothari, Luke Schaeffer, and Avishay Tal. Exponential separation between shallow quantum circuits and unbounded fan-in shallow classical circuits. In *Proceedings of the 51st Annual ACM SIGACT Symposium on Theory of Computing*, pages 515–526, 2019.

A Preliminaries

A.1 Classical circuit classes

Circuit classes form a crucial aspect of computational theory, helping to categorize and understand the computational capabilities of various models. Certain classical circuit classes emerge as especially relevant when studying constant-depth quantum circuits. This subsection will list and define the main classes of interest while also summarizing pertinent theorems associated with them.

Definition 32 (NC^k class). *The NC^k class is defined as the computational problems that can be solved in poly-logarithmic depth $\log(n)^k$ using polynomially-many gates. The gate set for this class comprises the following bounded fan-in gates,*

$$\left\{ \boxed{\text{AND}} \;,\; \boxed{\text{OR}} \;,\; \boxed{\text{NOT}} \right\} \;.$$

Definition 33 (AC^k class). *The AC^k class is defined as the computational problems that can be solved in poly-logarithmic depth $\log(n)^k$ using polynomial-many gates. The gate set for this class comprises the following unbounded fan-in gates,*

$$\left\{ \boxed{\text{AND}} \;,\; \boxed{\text{OR}} \;,\; \boxed{\text{NOT}} \right\} \;.$$

Definition 34. ($\mathsf{AC}^k[p]$ class). *The $\mathsf{AC}^k[p]$ class is defined as the computational problems that can be solved in poly-logarithmic depth $\log(n)^k$ using polynomial-many gates. The gate set for this class comprises the following unbounded fan-in gates,*

$$\left\{ \boxed{\text{AND}} \;,\; \boxed{\text{OR}} \;,\; \boxed{\text{MOD}_p} \;,\; \boxed{\text{NOT}} \right\} \;,$$

with MOD_p gate defined as follows,

$$\mathsf{MOD_p}(x) = \begin{cases} 1 & \text{if } \sum_{i=1}^n x_i \mod p = 0 \\ 0 & \text{if } \sum_{i=1}^n x_i \mod p \neq 0 \end{cases}. \tag{75}$$

The Razborov-Smolensky separations between all the $\mathsf{AC}^0[p]$ classes will be fundamental to establishing new separations between these and quantum constant depth circuit classes.

Theorem 35. *[41] Let p be a prime number, and q is not a power of p, then computing MOD_p with a depth d, $\mathsf{AC}^0[q]$ circuit, requires $\exp(\Omega(n^{1/2d}))$ size.*

Furthermore, it should be noted that this theorem implies that when we construct a graph using the $\mathsf{AC}^0[q]$ classes as vertices and draw edges between pairs of classes that are not subsets of each other, we obtain a complete graph. Thus, for each edge, at least two problems distinguish one class from the other (see Figure 4).
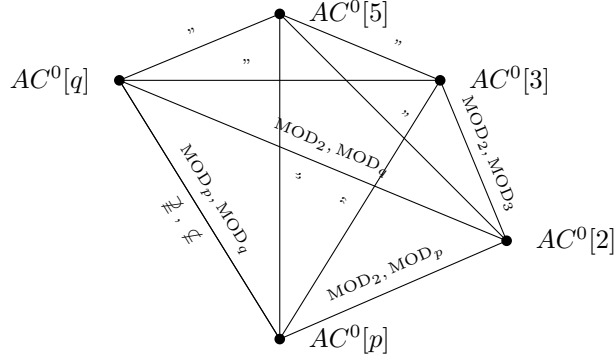
Figure 4: Graph representation of $\mathsf{AC}^0[p]$ classes with p prime. Each edge denotes that the connected classes are distinct, without one being a subset of the other. Along the edges, examples highlight problems that are in one class but excluded from the other.

Definition 36 (TC^k class). *The TC^k class is defined as the computational problems that can be solved in poly-logarithmic depth $\log(n)^k$ using polynomial-many gates. The gate set for this class comprises the following unbounded fan-in gates,*

$$\left\{ \boxed{\text{AND}} \ , \ \boxed{\text{OR}} \ , \ \boxed{\mathsf{TH}_t} \ , \ \boxed{\text{NOT}} \right\} \ ,$$

with TH_k gate defined as follows,

$$\mathsf{TH_t}(x) = \begin{cases} 1 & \text{if } \sum_{i=1}^n x_i \geq t \\ 0 & \text{if } \sum_{i=1}^n x_i < t \end{cases}. \tag{76}$$

We introduce a class that is not standard in circuit complexity literature but holds significance for the discussions and results presented in this text.

Definition 37. ($\mathsf{NC}^0[p]$ *class*). *The $\mathsf{NC}^k[p]$ class is defined as the computational problems that can be solved in poly-logarithmic depth $\log(n)^k$ using polynomial-many gates. The gate set for this class comprises the bounded fan-in AND, OR, NOT gates, and a single unbounded fan-in Mod p gates.*

A considerable number of important results in computational complexity pertain to the circuit classes we have defined, as well as their interrelations [15, 41, 39, 1]. Consequently, we will present the established containments for these classes,

$$\mathsf{NC}^0 \subsetneq \mathsf{AC}^0, \mathsf{NC}^0[p] \subsetneq \mathsf{AC}^0[p] \subsetneq \mathsf{TC}^0 \subseteq \mathsf{NC}^1. \tag{77}$$

This knowledge is crucial for comprehending the capabilities of each circuit class and discerning the position of quantum circuit classes relative to them.

Lastly, we will present the Vazirani-XOR lemma, which is of great interest to the study of parallel repeated games. This lemma is of particular interest for the analysis of constant-depth circuits and will be used to improve our classical hardness results.

Lemma 38. *(Vazirani's XOR Lemma [16]). Let D be a distribution on $\mathbb{F}_2^m$ and χ_S denote the parity function on the set $S \subseteq [m]$, defined as $\chi_S(x) = \oplus_{i \in S} x_i$. If $|\mathbb{E}_{x \in D}[(-1)^{\chi_S(x)}]| \leq \epsilon$ for every nonempty subset $S \subseteq [m]$, then D is $\epsilon \cdot 2^{m/2}$-close in statistical distance to the uniform distribution over $\mathbb{F}_2^m$.*

A.2 Quantum computation with qudits

We first review the basic operations on qudits, and then explain the qudit MBQC model.

A.2.1 Qudit operations

In this preliminary section, we present the qudit gates that will be employed in subsequent sections of the text to construct the quantum circuits essential for our main proofs.

The first qudit operation that we will define will be a generalized version of the qubit X gate.

Definition 39 (X qudit gate). *The* X *gate for qudits is defined as follows,*

$$\mathsf{X}_d \left| m \right\rangle := \left| m + 1 \mod d \right\rangle . \tag{78}$$

Then a rotation about the Z axis will be defined as follows,

Definition 40 (Rotation Z qudit gate). *The rotation Z operator for qudits is defined as follows,*

$$\mathsf{R}_Z^d(\phi) := \sum_{j=0}^{d-1} e^{i(1-sgn(d-1-j)\phi)} \left| j \right\rangle \left\langle j \right| . \tag{79}$$

In addition, we will define and make use of a more complex rotation Z operator.

Definition 41 (Generalized rotation Z qudit gate). *The generalized rotation Z operator for qudits is defined as follows,*

$$\mathsf{GR}_Z^d(\phi) := \sum_{j=0}^{d-1} e^{i(\phi j)} \left| j \right\rangle \left\langle j \right| . \tag{80}$$

The last single qudit operation will be the qudit Hadamard gate.

Definition 42 (Fourier gate). *The Fourier gate is defined as follows*

$$\mathsf{F}_d \left| m \right\rangle = \frac{1}{\sqrt{d}} \sum_{n \in \mathbb{Z}_d} w^{mn} \left| n \right\rangle , \tag{81}$$

with $w = e^{i\frac{2\pi}{d}}$.

Now the respective two qudit gates of interest are the qudit CNOT gate and the controlled rotation Z gate.

Definition 43 (SUM gate). *The* SUM *gate is defined as follows,*

$$\mathsf{SUM} \left| n \right\rangle \left| m \right\rangle = \left| n \right\rangle \left| n + m \right\rangle . \tag{82}$$

Definition 44 (Controlled generalized rotation Z qudit gate). *The* CGR_Z^d *gate is defined as follows,*

$$\mathsf{CGR}_Z^d \left| n \right\rangle \left| m \right\rangle = \left| n \right\rangle (\mathsf{GR}_Z^d)^n \left| m \right\rangle . \tag{83}$$

The last two multi-qudit operations are the following.

Definition 45 (fanout_p^{-1}). *The* fanout_p^{-1} *gate is defined as follows,*

$$\mathsf{fanout}_p^{-1} \left| x_0, x_1, \ldots, x_n \right\rangle := \left| x_0, (p - x_0) + x_1 \mod p, \ldots, (p - x_0) + x_n \mod p \right\rangle , \tag{84}$$

and can be implemented with $(\mathsf{fanout}_p)^{p-1}$.

Definition 46 (qMOD_p^{-1}). *The* qMOD_p^{-1} *gate is defined as follows,*

$$\mathsf{qMOD}_p^{-1} \left| x_0, x_1, \ldots, x_n \right\rangle := \left| x_0 + (p - x_1 + \ldots + x_n) \mod p, x_1, \ldots, x_n \mod p \right\rangle , \tag{85}$$

and can be implemented with $(\mathsf{qMOD}_p)^{p-1}$.

A.2.2 Qudit MBQC

The measurement-based quantum computation (MBQC) model was first introduced in [35, 36]. Unlike the standard circuit model, MBQC operates by performing measurements on universal quantum resource states [43]. Although these two models have a very different nature, they are computationally equivalent modulo a polynomial overhead. In this work, the generalization of MBQC to qudits [5] is especially relevant, since the circuits arising from this model exactly characterize the circuit classes, which we will analyze in detail.

In qudit MBQC, quantum algorithms are commonly referred to as *measurement patterns*. These patterns are defined by both a resource state and a distinct set of measurement operators for each qudit in the resource state. A noteworthy aspect is the existence of adaptivity, defined by the interdependencies between the measurement operators and their resulting outcomes. These interdependencies guide the information flow within the quantum state, which experiences decoherence due to the measurements; this guiding principle is termed 'flow.' This flow can be succinctly represented as a directed graph, denoted as $G = (V, E)$, where the vertices are associated with the measurement operators, and the update conditions between operators and results are represented by the edges of the graph [12]. The steps for executing a *measurement pattern* are detailed below,

1. Initialize a set of qudits, the number of which matches the count of vertices $|V|$ in the graph, all set to the state $F_p |0\rangle$;

2. Apply the entangling gates E_{v_i,v_j} between the necessary qudits to produce the resource state.

3. For each temporal layer t_i in the flow, sequentially:

   (a) Implement the Pauli corrections for each vertex in t_i, based on prior measurement outcomes $M_{j<i}$ as dictated by the edges of graph G.

   (b) Conduct the qudit measurement $M_{t_i}^b(\theta)$ within the same temporal layer t_i of the flow graph, for every time step i.

This model has been both the focus and inspiration for various works in studying the complexity of constant-depth quantum circuits [19, 11, 40]. However, a detailed analysis exploring the computational differences within the model, especially concerning the utilization of higher-dimensional resource states and measurement operators, remained to be delved into [5].

A.3 Quantum circuit classes with infinite gatesets

Definition 47 (i-**QNC$_d^0$**). *For a given positive integer d, let $\mathcal{U}_d$ represent the set of all unitary operators on a d-dimensional Hilbert space $\mathcal{H}^d$, and let $\mathcal{C}_d$ denote the set of single qudit controlled gates from $\mathcal{U}_d$. We define* i-QNC$_d^0$ *as the class of quantum circuits with constant depth and polynomial size, using a gate set drawn from the combination of $\mathcal{U}_d$ and $\mathcal{C}_d$.*

Definition 48 (i-**QAC$_d^0$**). *For a given positive integer d, let $\mathcal{U}_d$ represent all unitary operators on a d-dimensional Hilbert space $\mathcal{H}^d$, and let $\mathcal{T}_d^k$ denote a multi-qudit controlled gate selected from $\mathcal{U}_d$. We define* i-QAC$_d^0$ *as the class of quantum circuits with a constant depth and polynomial size, using a gate set drawn from the combination of $\mathcal{U}_d$ and $\mathcal{T}_d^k$ with unbounded classical fanout.*